

**DESIGN AND TESTING OF A MULTI-PARAMETRIC PERFUSION
BIOREACTOR FOR RAT ABDOMINAL WALL VASCULARIZED
COMPOSITE ALLOGRAFT PRESERVATION**

By

Kenny Tran

A thesis submitted to Johns Hopkins University in conformity with the requirements for the
degree of Master of Science in Biomedical Engineering

Baltimore, Maryland

May, 2018

ABSTRACT

Organ transplantation is a method of treating diseases and restoring organ function that involves procuring an organ from a donor and transplanting it into a recipient. Due to the success and growth of this field of treatment, there is a large demand for available organs. However, there is a vast difference between the number of available organs and patients waiting for an organ. In 2013, there were 121,272 patients on the waitlist for an organ donation but only 28,954 organs were transplanted that year. In order to combat the discrepancy between those two numbers, the field of organ transplantation is turning to organ preservation. At first, static cold storage was used to lower the metabolic rate of the organs and thus preserve them. However, that technique still caused hypoxic damage to the organs. Thus the use of organ perfusion systems became more common for organ preservation. Even though there are several commercialized perfusion systems for traditional organs, there are no specialized systems for vascularized composite allografts (VCA). Unlike traditional solid organs, VCA are composed of multiple tissue types (i.e. skin, muscle, and bone). Examples of VCA are hand or face transplants. Even though these types of transplants are not considered life-saving, they can be considered as life-restoring.

Here we describe the design of a bioreactor system that is capable of maintaining the rat abdominal wall VCA. This type of model is chosen because abdominal wall transplants are the second most common type of VCA. The bioreactor system will store the abdominal wall in a safe and sterile environment while allowing for the perfusion of the tissue with a specialized organ solution simultaneously with electrical stimulation. This bioreactor system will contain various sensors, including pressure, oxygen, pH, and temperature, to monitor the viability of the abdominal wall throughout the perfusion. With this bioreactor, many more studies on the preservation of VCA can be performed, with the eventual goal of increasing the current gold standard's maximum preservation time of 4-6 hours to eventually 72 hours.

Thesis Readers:

Dr. Warren L. Grayson, Ph.D., Dr. Gerald Brandacher, MD., Dr. Kevin J. Yarema, Ph.D.

ACKNOWLEDGEMENTS

I would like to first thank myself for being me. Also anime. I could not have done it without you.

On a more serious note, I would like to first thank my advisor Dr. Warren Grayson for accepting me into his lab despite my lack of research experience. His guidance throughout this project has been very helpful. I would also like to thank Sara Salehi and Vanessa Guarnizo for providing me with the rat abdominal walls needed for my experiments as well as their assistance and feedback on the design of the bioreactor. Sarah Somers and Ashley Farris also provided valuable feedback and assistance on the bioreactor design, electrical stimulation system, and oxygen probes. For that I am forever thankful. The other members of the Grayson lab have also helped in tangible and intangible ways, whether it be academically or socially. Thus, I would like to thank Jordie Gilbert, Dr. Dennis Lambrechts, Dr. Justin Morrisette-McAlmon, Ethan Nyberg, Lexi Rindone, and Makeda Stephenson. I am grateful to have met these members of the Grayson Lab and I wish them the best of luck in the rest of their careers.

I would also like to thank my family for their continued love and support throughout my Masters career. Without my parents' support and guidance, I would not be where I am today. In addition to my parents, I also want to thank all of the friends that I have made. Our experiences together have helped shape me into the person that I am today and I hope that we can maintain our friendship for many more years to come.

TABLE OF CONTENTS

| | |
|---|------------|
| ABSTRACT | ii |
| ACKNOWLEDGEMENTS | iii |
| TABLE OF CONTENTS | iv |
| LIST OF TABLES | vi |
| LIST OF FIGURES | vii |
| CHAPTER 1: TRANSPLANTATION AND PRESERVATION | 1 |
| 1.1 Organ Transplants and Vascularized Composite Allografts (VCA) | 1 |
| 1.2 Organ Preservation | 4 |
| 1.3 Perfusion Systems | 8 |
| 1.3.1 Solid Organs | 10 |
| 1.3.2 Vascularized Composite Allografts | 13 |
| 1.3.3 Limitations of Other Perfusion Systems | 15 |
| CHAPTER 2: RAT ABDOMINAL WALL VCA MODEL | 17 |
| 2.1 The Rat Abdominal Wall | 17 |
| 2.2 Harvesting and Perfusing the Abdominal Wall VCA | 17 |
| 2.3 Model for Transplantation | 20 |
| CHAPTER 3: BIOREACTOR HOUSING AND DESIGN | 22 |
| 3.1 Bioreactor Housing Design and Fabrication | 22 |
| 3.2 Bioreactor Prototype | 28 |
| 3.3 Sterile Assembly | 31 |
| CHAPTER 4: PERFUSION TESTS | 33 |
| 4.1 Flow Through System | 33 |
| 4.1.1 Components of Flow Circuit | 33 |
| 4.1.2 Calibration of the Sensors | 36 |
| 4.2 Experimental Set Up and Methods | 37 |
| 4.3 Results | 39 |
| 4.4 Discussion | 42 |
| CHAPTER 5: ELECTRICAL STIMULATION | 45 |
| 5.1 Electrical Stimulation Background | 45 |
| 5.2 Circuit Design and Theory | 45 |
| 5.3 Experimental Set Up and Methods | 49 |
| 5.3.1 Electrical Stimulation Experiment 1: Proof of Concept | 50 |
| 5.3.2 Electrical Stimulation Experiment 2: Within the Bioreactor | 51 |
| 5.4 Results | 52 |
| 5.4.1 Electrical Stimulation Experiment 1 Results | 52 |
| 5.4.2 Electrical Stimulation Experiment 2 Results | 53 |
| 5.5 Discussion | 54 |
| CHAPTER 6: CONCLUSIONS | 56 |
| REFERENCES | 58 |
| APPENDICES | 62 |
| List of Materials for Bioreactor | 62 |
| Arduino Code: Electrical Stimulation | 63 |

| | |
|--|-----------|
| <i>MATLAB Code: Measuring the Percent Area of Contraction Upon Stimulation</i> | <i>63</i> |
| <i>MATLAB Code & GUI: Automation of the Pump</i> | <i>65</i> |
| CURRICULUM VITAE..... | 71 |

LIST OF TABLES

CHAPTER 1

| | |
|---|----|
| Table 1.1: Commercialized Perfusion Systems | 11 |
|---|----|

CHAPTER 3

| | |
|---|----|
| Table 3.1 The Range and Accuracies of the MLT1030/D | 26 |
|---|----|

LIST OF FIGURES

CHAPTER 1

| | |
|---|----|
| Figure 1.1 Trend for Organ Transplant Waiting List, Transplants, and Organ Donors..... | 2 |
| Figure 1.2 Common Maximum Ischemia Times for Various Organs | 3 |
| Figure 1.3 Artistic Representation of Multiparametric Bioreactor | 16 |

CHAPTER 2

| | |
|--|----|
| Figure 2.1 Experimental Rat VCA Models..... | 17 |
| Figure 2.2 Anesthetized Rat with Shaved and Marked Abdomen | 18 |
| Figure 2.3 The Abdomen with Cut Skin and Cauterized Edges | 19 |
| Figure 2.4 The Harvested Abdominal Wall with Intact Vessels..... | 20 |
| Figure 2.5 The Reduced Graft Sizes | 21 |
| Figure 2.6 A Rat Abdominal Wall Transplant 5 Days Post-Surgery..... | 21 |

CHAPTER 3

| | |
|--|----|
| Figure 3.1 Overall Bioreactor Design in Solidworks..... | 23 |
| Figure 3.2 Top Down View of Bioreactor | 23 |
| Figure 3.3 Inner Space of Bioreactor | 24 |
| Figure 3.4 The MLT1030/D Force Transducer with the 5 Blades Fanned Out..... | 25 |
| Figure 3.5 The Method of Connecting the Tissue to Force Sensor | 25 |
| Figure 3.6 Close Ups of the Tissue Holder Platform and Drainage Perfusate Reservoir | 27 |
| Figure 3.7 The Four Removable Sliding Panels | 28 |
| Figure 3.8 Side Views of Closed 3D Printed Bioreactor Prototype..... | 29 |
| Figure 3.9 Close Up of Perfusion Ports and Electrode Tab | 29 |
| Figure 3.10 Front View of Opened 3D Printed Bioreactor Prototype | 30 |
| Figure 3.11 Top Down View of Opened 3D Printed Bioreactor Prototype..... | 30 |
| Figure 3.12 Close Up of Perfusate Drainage Well..... | 31 |
| Figure 3.13 Exploded View of Bioreactor | 32 |

CHAPTER 4

| | |
|---|----|
| Figure 4.1 Flow Circuit Diagram | 33 |
| Figure 4.2 The Ismatec IP 8 Peristaltic Pump..... | 34 |
| Figure 4.3 Main Perfusate Reservoir with a Mix of Evans Blue Dye and Saline..... | 34 |
| Figure 4.4 An Ion Sensor with a Flow Through Fitting..... | 35 |
| Figure 4.5 The PowerLab with Two Accompanying Bridge Amplifiers | 36 |
| Figure 4.6 Flow Through Sensor Graph Readings from LabChart..... | 37 |
| Figure 4.7 How the Tissue is Attached to the Force Sensor | 38 |
| Figure 4.8 The Perfusion System Connected to the Bioreactor Prototype | 39 |
| Figure 4.9 Perfusion of the Abdominal Wall with Evans Blue Dye..... | 40 |
| Figure 4.10 Pressure Readings..... | 40 |
| Figure 4.11 Temperature Readings | 41 |
| Figure 4.12 Percent Oxygen Readings..... | 41 |
| Figure 4.13 Percent pH Readings | 42 |
| Figure 4.14 Air Bubbles in the Outflow Tubing..... | 42 |
| Figure 4.15 Perfusate Reservoir with Mixed Saline | 42 |

CHAPTER 5

| | |
|--|----|
| Figure 5.1 Schematics of P-Channel and N-Channel MOSFETs | 46 |
| Figure 5.2 H-Bridge Circuit Schematic. | 47 |
| Figure 5.3 The Two Possible Orientations of the H-Bridge Circuit. | 48 |
| Figure 5.4 The Output Waveform from the H-Bridge Circuit..... | 49 |
| Figure 5.5 Electrical Stimulation Set Up | 50 |
| Figure 5.6 Experiment 1: Frames of the Tissue when Unstimulated and Stimulated..... | 52 |
| Figure 5.7 Different Stages of the Video Analyzing Process | 52 |
| Figure 5.8 Experiment 2: Frames of the Tissue when Unstimulated and Stimulated..... | 53 |
| Figure 5.9 Experiment 2: Force Measurement Readings..... | 54 |

Note to Reader: Some parts of Chapter 1 were taken from an unpublished review article that I co-authored.

CHAPTER 1: TRANSPLANTATION AND PRESERVATION

1.1 Organ Transplants and Vascularized Composite Allografts (VCA)

Organ transplantation to treat diseases and restore organ function is not a new concept. Throughout history and even religious texts, there have been stories of organs or tissues being transplanted, but it was not until 1883 that Theodor Kocher successfully transplanted thyroid tissue from one patient into another [1]. His work with the thyroid transplants would lead to the growth of organ transplantation as an accepted method of treatment for organ failure. Throughout the years, there would be an increased number of organ transplant surgeries and new developments such as Alexis Carrel and Charles Guthrie's first heart transplant in a dog model in 1905 [1]. However, those transplants would eventually fail due to the recipient's immune response and rejection of transplanted organ [2]. It would not be until 1954 that the first successful human kidney transplant was performed by Dr. Joseph Murray and John Merrill and 1967 that the first successful human heart transplant would be completed by Dr. Christian Barnard [2, 3].

As the strategies for immunosuppression for organ transplants became better defined and the number of organ transplants began to rise, the number of available organs from organ donors would also rise as new legislation changed the definition of brain death, the timing and techniques of organ procurement from donors, and extended organ donor criteria. However, the number of patients waiting for organ transplants would increase at a much greater rate than the slowly growing number of available organs. This trend can be seen in **Figure 1.1**.

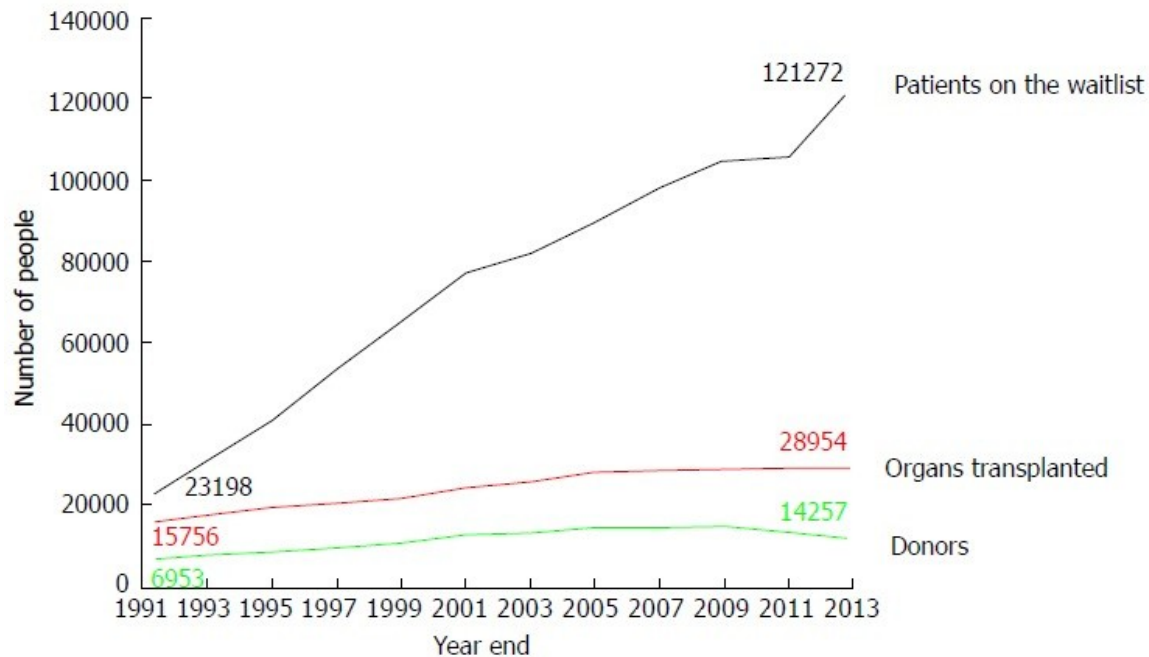


Figure 1.1 Trend for Organ Transplant Waiting List, Transplants, and Organ Donors [4]

Since there is an ever growing number of patients waiting for an organ donation, there is an increasing need to obtain more organs that are viable for transplantation. Even after an organ is procured from a donor, it is not always transplanted into a recipient. For example, about 20% of kidneys (totaling 3159) that were obtained for transplantation were discarded in 2015 [5]. Even though some of those organs may be discarded because they are physically unfit for donation, many become damaged during transport, or some organs are discarded because they cannot be matched to a suitable recipient within a certain time period [4]. After an organ is obtained from a donor, it is matched to a suitable recipient based on factors such as blood type, the physical characteristics of the organ, the patient's medical condition, and even distance between the donated organ and recipient [6]. If a recipient is found, the organ is stored in a bag of chilled preservation solution over ice, which is the current gold standard for organ preservation, and transported to the recipient. During transport, the organ is cut off from any oxygen supply and suffers from ischemia – the deprivation of oxygen, and glucose supply to the

organ – which leads to degradation of the organ. **Figure 1.2** lists the maximum allowable cold ischemia time for various organs. During that period of maximum allowable ischemia time, the organ needs to be matched to an appropriate recipient, transported to that recipient, and transplanted into the recipient.

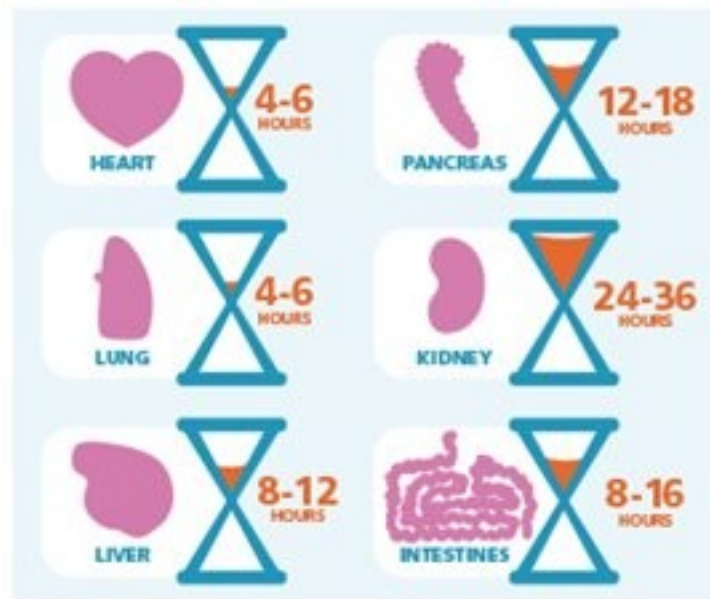


Figure 1.2 Common Maximum Ischemia Times for Various Organs [6]

With the success and growth of the solid organ transplantation field, the number of Vascularized Composite Allotransplantations or Vascularized Composite Allografts (VCA) is also increasing. VCA are composed of multiple tissue types such as skin, muscle, and bone and are used to replace tissue defects that cannot be reconstructed, such as those lost due to trauma or accidents [7]. Examples of these can be seen in face or limb transplantations [8]. Even though these transplants are not considered lifesaving surgeries, they can be seen as “life-restoring” since they allow for restoration of both function and aesthetics when compared to autologous tissue reconstructions and prosthetics [8]. Due to their composite nature, VCA require a wider range of immunosuppressants due to the immunogenicity of skin and have limited preservation times of 4-6 hours due to the skeletal muscle component [7]. In the United States, traumatic

amputation is the second leading cause of limb loss and over 100 limb transplants have been performed worldwide since 1999 [9]. In 2013, the United States Department of Health and Human Services (HSS) stated that VCA are designated as organs and they will be regulated by the Organ Procurement and Transplant Network (OPTN) together with the United Network for Organ Sharing (UNOS) [10]. Like the other organs of conventional organ transplants, VCA also suffer from ischemia during transportation times and methods of combating the ischemia is being researched.

1.2 Organ Preservation

The goal of organ preservation is to maintain the viability and function of the organ outside of the body. Without the rest of the body to provide an adequate supply of oxygen, glucose, other nutrients, and metabolic waste removal through blood flow, the body undergoes ischemia. During ischemia, the cells switch from producing ATP via oxidative metabolism to anaerobic metabolism, which is less efficient [11]. The use of anaerobic metabolism leads to the buildup of metabolites such as lactic acid, which lowers the cellular pH and other changes, which affects the function of enzymes and both the mitochondrial and cellular membrane pumps [11]. Ischemia and anaerobic metabolism affects the electrolyte concentration, which causes a shift in the oncotic pressure, leading to cellular swelling, rupture, and cellular apoptosis [11]. Reactive oxygen species (ROS), such as NADPH oxidase (NOX) are also produced during ischemia and anaerobic metabolism, which affects the function of the mitochondria and can lead to a reciprocal production of more ROS [11].

Ischemia-reperfusion injury is an autoimmune event that occurs due to a restoration of blood flow after a period of ischemia [12]. With the restoration of blood flow, there is also a restoration of oxygen and glucose supply, which allows the cells to switch back to oxidative

metabolism [11]. But this leads to a large increase in ROS production since the mitochondria's mechanisms for oxidative metabolism are damaged during ischemia [11]. The addition of ROS leads to the disruption of the mitochondrial membrane and the release of mitochondria-specific proteins into the cytosol, which triggers apoptosis and the activation of the innate immune system [11]. Even though the immune system normally is needed for regeneration and healing, during ischemic reperfusion injury (IRI), both injured and dead cells release molecules that cause them to be attacked by neutrophils [11]. This can lead to a cascade of events and may ultimately result in organ failure [12]. Nitric oxide (NO) levels are also affected by the buildup of ROS, which leads to deactivation of adhesion molecules on the surfaces of cells, leading to the transmigration of immune cells to other parts of the body [11].

In addition to causing organ failure, ischemia-reperfusion injury in transplanted tissues and organs can also lead to acute rejection or affect the long-term recipient's acceptance of the transplant [8]. In 2010, Shimizu *et al* found that transplants that underwent longer periods of ischemia resulted in a more severe rejection of the tissue [13]. Thus, the goal of organ preservation is to limit the period of ischemia time in order to reduce the effects of ischemia-reperfusion injury.

There are two overarching strategies for organ preservation: 1. Suppression of the organ's metabolism using hypothermic conditions and 2. Replacing the physiological environment through normothermic environments and biophysical stimulation.

The current gold standard of organ preservation is to store the organ within a chilled and specialized preservation solution during transport, which is known as static cold storage. Static cold storage lowers the temperature of the organ to about 0-4°C to lower the metabolic demand of the organ during transport. For every 10°C in temperature, there is a 50% decrease in

metabolic rate, eventually resulting in a metabolic rate of 10-12% of normal physiological levels at 4°C [14]. Even though the metabolic demand is lower, organs undergoing static cold storage still suffer from oxidative stress, the production of ROS, and inflammation [15].

Specialized preservation solutions were developed to help combat the molecular changes in the organs. One of the first solutions to be developed was the EuroCollins solutions in the 1980s. It is a solution that uses a high potassium ion concentration as an osmotic barrier and glucose [15]. Even though it was successfully used to preserve kidneys, hearts, livers, and lungs, the preservation times of those organs using this solution was also lowered [15]. Since the glucose was converted to lactate and resulted in acidosis, the solution was later modified to use sucrose or mannitol instead of glucose [15]. The University of Wisconsin (UW) solution was also developed in the 1980s and is used as the gold standard for liver grafts since [15]. It works by 1. Preventing edema, 2. Supplying the cells with adenosine, the precursor of ATP, and 3) Providing antioxidant defense while being able to be used with multiple types of tissues since its components are all metabolically inert [15]. Histidine-Tryptophan-Ketoglutarate (HTK) is another commonly used preservation that uses its histidine content to augment the osmotic effect of mannitol to prevent edema, tryptophan to stabilize cellular membranes and to prevent histidine from entering cells, and ketoglutarate as a substrate for anaerobic metabolism during perfusion [16].

Even though static cold storage is able to lower the metabolic demands of the organs during preservation, there is still a metabolic demand for oxygen and glucose. The organs are submerged in preservation solutions that contain oxygen and other substrates for metabolism, yet the slow diffusion rate of oxygen and those substrates through the tissue prevents an adequate supply of oxygen and metabolic substrates into the deeper regions of the tissue. Thus, the field

has turned to machine perfusion of the organs to deliver the necessary nutrients throughout the rest of the organ.

The idea of perfusing organs outside of the body is not new: in 1812, the physiologist Le Gallois once wrote that “if one could substitute for the heart a kind of injection... of arterial blood, either naturally or artificially made, ... one would succeed easily in maintaining alive indefinitely any part of the body whatsoever” [17]. In other words, he theorized that it is possible to preserve an organ outside of the body as long as the physiological environment of the organ can be mimicked.

Even though the concept of organ preservation via perfusion has been around for a while and there were a few rudimentary attempts at ex-vivo organ perfusion, it was not until 1935 when an entire system was created for organ perfusion. In 1935, Alexis Carrel created a setup that was able to perfuse ovaries, adrenal glands, thyroid glands, spleens, hearts, or kidneys from a cat or fowl [18]. By pumping perfusate throughout the organ, Carrel *et al* were able to provide sufficient nutrient and oxygen delivery throughout the organs and extend their preservation times.

The dual approach to organ preservation through hypothermic machine perfusion (HMP) has been well studied and is traditionally more common compared to normothermic machine perfusion (NMP), which uses temperatures from 12-37°C. For examples, kidneys have been successfully transplanted even after 24 hours of hypothermic machine perfusion [19]. Even though hypothermic preservation is capable of prolonging organ preservation times, normothermic preservation provides inherent advantages over hypothermic conditions. With hypothermic preservation, there will always be a maximum preservation time, hypothermia affects cell and organ function so it does not allow for viability and functional assessments of the

organ, and the organs will suffer from hypothermic preservation damage as they are being preserved for longer periods of time [19]. Since the organ donor criteria has expanded in order to meet the ever growing demand for organs, organs that would have been discarded before are now being used for transplantation. Those organs are often sensitive to hypothermia and are not able to survive the damage that hypothermic preservation causes [19]. By using normothermic preservation, it is theoretically possible to avoid the disadvantages of hypothermic preservation. It allows for the storage of organs in a metabolically active state by providing oxygen and nutrients without cooling. Normothermic preservation would also allow for the function and viability of organs to be assessed during preservation and can possibly recover organs that are considered “marginal” or injured [19].

1.3 Perfusion Systems

The components of Alexis Carrel’s *ex-vivo* organ perfusion system are still commonly used in the contemporary perfusion systems. Their set up contained 1) a housing chamber to maintain a sterile environment for the organ, 2) a perfusate medium that would supply a sufficient amount of oxygen and nutrients to the organ, 3) a way to replenish the amount of oxygen in the perfusate, and 4) phenol red was also added to the perfusate as a non-invasive way to monitor the pH and thus the metabolic activity of the organ.

Even though they were able to perfuse various organs for a longer period of time, there were still various limitations with their system. For example, their system did not have a way to measure viability of the organ or its function besides using phenol red to give a relative measurement of pH changes. In their paper, the authors also describe how the organs often had a large increase in weight and the authors credited that to tissue growth and generation from the perfusion [18]. However, many recent studies have shown that the weight gain is a byproduct of

edema, not tissue growth. Even though there are short-comings with Carrel's 1935 perfusion system, many perfusion systems of today also incorporate similar components into their systems: a Housing System, Perfusate, a Perfusion Loop, and Non-Invasive Measurement Methods.

Housing systems provide a closed and sterile environment to protect the organ from bacterial infections and provide a reproducible way for the perfusion system to connect to the organ. They also maintain the hydration of the tissue or organ.

Perfusates are pumped throughout the organ to provide oxygen and other nutrients for metabolism. There are several specialized perfusates such as the previously mentioned EuroCollins and University of Wisconsin solutions. Each solution has its own unique additives in order to attenuate organ damage during perfusion. For example, several preservation solutions contain additives to control the osmolality of the solution to prevent swelling in the organ.

Perfusion Loops contain pumps and other devices for pressure-driven flow of the perfusate through the organ. Key elements of perfusion loops include a pump, oxygenator, perfusate reservoir, heat exchangers, tubing, and sensors. The pump drives the perfusate. The oxygenator replenishes the oxygen supply in the perfusate to promote aerobic metabolism in the organ. The reservoir stores excess perfusate to essentially provide a semi-batch process where the perfusate only needs to be replenished intermittently. Heat exchangers or temperature controllers are used to adjust the temperature of the perfusate as needed for either hypothermic or normothermic perfusion. The tubing connects the different components of the perfusion loop and houses the flow through sensors for measurement of various perfusate parameters such as pressure. In order to prevent pressure related damage to the organs, many perfusion systems operate at pressures that are lower than physiological levels (80-120 mmHg for humans) [20]. An example of these components can be seen in OrganOx's meta normothermic liver perfusion

devices. It contains a perfusion pump that maintains the hepatic artery pressure between 60-75 mmHg, an oxygenator that keeps the respective partial pressures of oxygen and carbon dioxide at 12 kPa and 5 kPa respectively, and a heat exchanger to maintain the perfusate temperature at 37°C [21].

Non-invasive measurements allow for continuous and automatic measurements of the perfusate and the organ for monitoring of the organ's functions and viability. Perfusion systems commonly include pressure, flow rate, temperature, pH, and oxygen sensors. Other sensors can include glucose and lactate sensors in order to monitor the metabolism of the organ. Perfusion systems that are specialized for a type of organ can include sensors that can monitor a specific function of that organ. For example, Transmedic's Organ Care System for the Heart allows for the continuous monitoring of heart rate via an electrocardiogram while checking for any fibrillations of the heart during preservation and transport [22]. It also includes an electrode to measure the heart's electrocardiogram and R-wave to adjust the pump speed and thus pump stroke volume as needed to maintain a continuous flow in the system [22].

1.3.1 Solid Organs

Over the past couple of decades, several companies developed specialized systems for the perfusion and preservation of various organs. The following table lists commercially available perfusion systems for the heart, lungs, kidneys, and liver.

Table 1.1: Commercialized Perfusion Systems

| Organ | Company Device | Common Features | Unique Features |
|-------|--|---|---|
| Heart | Organ Transport Systems Life Cradle [23][24] | <ul style="list-style-type: none"> • Safe organ storage • Maintains oxygen in perfusion • Monitors Temperature • Oxygenates perfusion solution • Transportable | <ul style="list-style-type: none"> • Uses preservation solution • Hypothermic Perfusion (5°C) |
| | Paragonix SherpaPerfusion Cardiac Transport System [25] | | <ul style="list-style-type: none"> • Uses preservation solution • Hypothermic perfusion (4-8°C) • Monitors ischemia time • Low pressure perfusion (4-6 mmHg) • Can communicate with mobile devices • Single-use, disposable system |
| | Transmedics Organ Care System Heart [22][26] | | <ul style="list-style-type: none"> • Uses donor blood + solution mix • Normothermic Perfusion • Monitors organ function. Such as aortic pressure, coronary flow, heart rate, blood temperature • Housing enables ultrasound assessment and blood sampling • Console is reusable, but perfusion set is one-time use |
| Lung | Organ Assist Lung Assist [27] | <ul style="list-style-type: none"> • Safe organ storage • Ventilates organ • Allows for oxygenation and deoxygenation of perfusate for evaluation of lungs | <ul style="list-style-type: none"> • Uses preservation solution • Temperature controllable: 10-38°C • Pumps output up to 20 mmHg and 5L/min |
| | Transmedics Organ Care System Lung [28] | | <ul style="list-style-type: none"> • Uses donor blood + solution mix • Normothermic Perfusion • Enables ultrasound assessment and blood sampling • Console is reusable, but perfusion set is one-time use • Transportable |

| | | | |
|--------|--|---|--|
| | XVIVO Perfusion Xvivo Lung Perfusion System (XPS) and Disposable Lung Set (DLS) [29] | | <ul style="list-style-type: none"> • Uses preservation solution • Temperature controllable 15-39°C • Monitors pO₂ and pH of perfusate • Allows for X ray • XPS is reusable, but requires single use DLS |
| Kidney | Organ Recovery Systems LifePort Kidney Transporter [30] | <ul style="list-style-type: none"> • Safe organ storage • Uses preservation solution • Transportable | <ul style="list-style-type: none"> • Hypothermic perfusion (uses ice) • Monitors: temperature, flow rate, vascular resistance, and pressure • System is reusable, perfusion kit is single use |
| | Organ Assist Kidney Assist (Transport) [31] | | <ul style="list-style-type: none"> • Temperature control 10-38°C • Transportable version only supports 0 - 4°C • Oxygenates solution • Outputs flow, temperature, and pressure readings • Pumps output up to 20 mmHg and 5L/min |
| | Waters Medical Systems Wave or RM3 [32][33] | | <ul style="list-style-type: none"> • Hypothermic perfusion (3-10°C) • Oxygenates solution • Outputs 0-250 mL/min flow • Monitors pressure, flow, temperature, and renal resistance • Control unit is reusable, cassette is disposable/single use • Can be connected to a network for online monitoring of data |
| Liver | Organ Recovery Systems LifePort Liver Transporter [34] | <ul style="list-style-type: none"> • Safe organ storage | <ul style="list-style-type: none"> • Uses preservation solution • Hypothermic perfusion • Monitors: temperature, flow rate, vascular resistance, and pressure • System is reusable, perfusion kit is single use • Small, lightweight, transportable |
| | Organ Assist Liver Assist [35] | | <ul style="list-style-type: none"> • Uses preservation solution • Temperature controllable 10-38°C • Oxygenates solution • Outputs flow, temperature, and pressure readings |

| | | | |
|--|--|--|---|
| | | | <ul style="list-style-type: none"> • Allows for sampling of perfusate and bile |
| | OrganOx Metra [36][21] | | <ul style="list-style-type: none"> • Uses blood • Normothermic perfusion • Maintains oxygen in perfusion • Measures pO₂, pCO₂, pH, temperature, glucose, bile production • Console is reusable but has a sterile disposable portion for single use • Large, but transportable |
| | Transmedics Organ Care System Liver [37][38] | | <ul style="list-style-type: none"> • Uses donor blood + solution mix • Normothermic Perfusion 34-37°C • Maintains oxygen in perfusion • Measures lactate in perfusate and bile production for evaluation • Enables ultrasound assessment and blood sampling • Console is reusable, but perfusion set is one-time use • Large but transportable |

1.3.2 Vascularized Composite Allografts

At the moment, there are not any commercially available perfusion systems for VCA perfusion and the current gold standard for preserving VCA involves static cold storage at around 0-4°C. Thus, these types of transplantations need to be done within 4-6 hours of ischemia. There is a trend towards researching and developing methods and devices for extracorporeal VCA perfusion. Two notable groups are the Ozer and Kueckelhaus groups.

In 2016, Kueckelhaus *et al* developed a mobile system that is use for perfusing porcine limbs. Their system uses a peristaltic pump to perfuse cool and oxygenated Perfadex solution into a porcine forelimb for 12 hours while taking measurements such as pressure, oxygen, and temperature and taking samples of the perfusate for blood gas analysis. Even though their perfused limbs had a significant amount of weight gain compared to limbs stored in static cold

storage, they were able to electrically stimulate their limbs for a longer amount of time into the perfusion. Histological analysis of the perfused limbs does not show hypoxic damage to the cells while the cold storage limbs do [9]. In 2017, they again compared their perfusion system to static cold storage by replanting the limb onto the donor pig after 12 hours of perfusion or 4 hours of cold storage. After replantation, they monitored the pigs for 7 days. They found that the control animals (limbs preserved with cold storage) had higher levels of potassium and myoglobin in their blood, which suggests muscular tissue damage. They also found that the expression of Hypoxia-inducible factor 1-alpha (HIF-1 α) and Hypoxia-inducible factor 1-beta (HIF-1 β) in the perfused limbs were comparable to fresh muscle tissue, which suggests the limbs were adequately oxygenated. One of the four pigs in the control group (static cold storage) died of pulmonary complications, which is a consequence of ischemia-reperfusion injury, while all of the 3 pigs in the treatment group (perfusion) survived past the 7-day mark [39].

In 2015, the Ozer group created their own porcine limb perfusion set up that perfused warm (27-32°C) autologous blood into the limbs instead of using a cool acellular solution like the Kueckelhaus group. After 12 hours of perfusion or 6 hours of static cold storage, the limbs were transplanted onto another pig host. They monitored the perfusion parameters such as temperature and pressure during perfusion, collected the perfusate for blood gas analysis, and checked for muscle contraction of muscle fiber bundles using a nerve stimulator. Even after 12 hours of perfusion, they found that the muscle fibers were still able to contract [40]. In a 2016 report, they used the same set up but perfused the porcine limbs for 24 hours instead of the 12 hours in the previous year. Once again, they found that the perfusion group had better results than the cold storage group since the muscle fibers were able to contract upon electrical stimulation after 24 hours of perfusion, indicating the presence of healthy myocyte units [41]. In

2017, the group reported on a perfusion set up of a human forelimb from brain dead adult donors for 24 hours. After perfusion, they performed histology on the muscle fibers of the limbs and found that there were no signs of necrosis, degeneration, or inflammatory cell infiltration. Also, they were able to stimulate and obtain contraction from both dissected single muscle fibers and the whole limb against gravity. Their findings indicate that they were able to use near-normothermic extracorporeal perfusion to preserve human VCA function for at least 24 hours [42].

1.3.3 Limitations of Other Perfusion Systems

Even though all of the perfusion systems mentioned in the previous sections are theoretically able to extend the preservation times of their organs, there are no systems that are designed specifically for VCA. The commercialized perfusion systems are designed for their specific organs such as the heart or lungs while the perfusion systems of the Kueckelhaus and Ozer groups are relatively primitive. While those systems are able to pump perfusate throughout the organ, there are no specialized sensors for monitoring VCA biomarkers to measure the function and viability of the organ. In our proposed system for rat abdominal wall perfusion, we will include specialized sensors that will be able to monitor the status of the abdominal wall along with an electrical stimulation system with force sensors to monitor the functionality of the tissue. **Figure 1.3** shows an artistic rendering of the proposed bioreactor system with the enclosed abdominal wall with an attached force sensor. Connected to the bioreactor is the flow through system with various flow through sensors and components such as the pump as well as the electrical stimulation system.

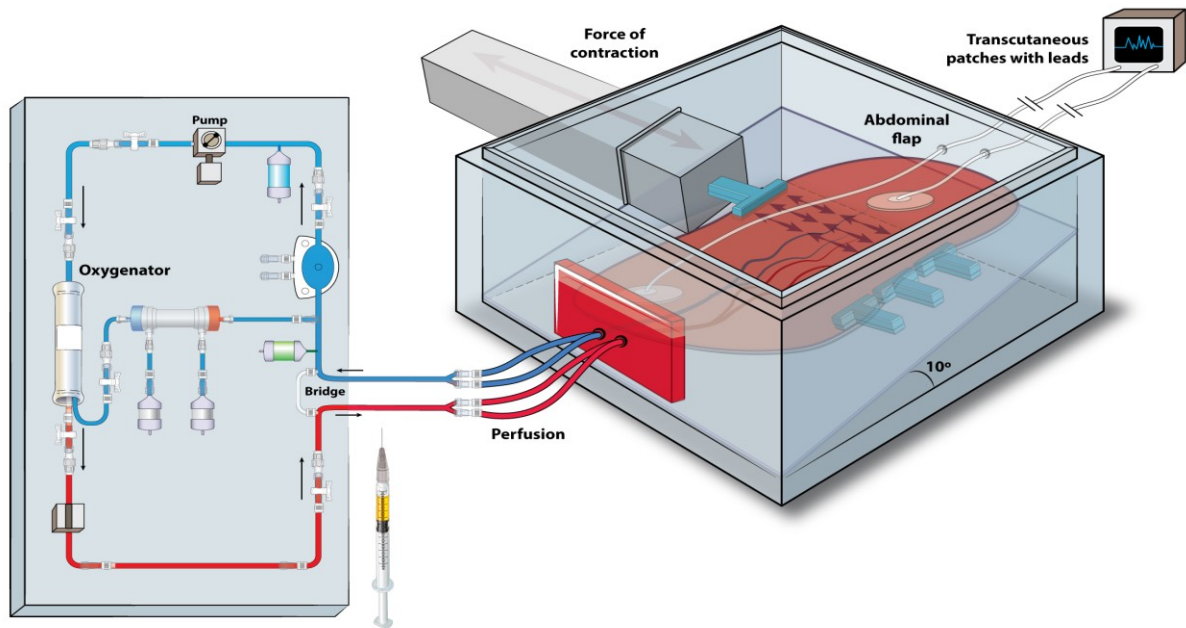


Figure 1.3 Artistic Representation of Multiparametric Bioreactor. In the center is the bioreactor housing with the embedded tissue graft, force sensor, and electrical stimulation system (Right). On the left is the perfusion circuit with the peristaltic pump, oxygenator, and various inline sensors.

CHAPTER 2: RAT ABDOMINAL WALL VCA MODEL

2.1 The Rat Abdominal Wall

With over 40 surgeries completed as of 2015, the abdominal wall transplant is the second most common form of VCA transplant [43]. The animal model this project focuses on is the rodent abdominal wall VCA model, which was pioneered by the Brandacher lab [43]. The abdominal wall is composed of three layers of muscles: the transverse abdominis, internal oblique, and external oblique and consists of multiple types of tissues: skin, muscle, and subcutaneous fat [44]. It is needed for many mechanical functions such as generating motions such as twisting, lateral bending, and flexion as well as maintaining spinal column stability and intra-abdominal pressure [44].

2.2 Harvesting and Perfusing the Abdominal Wall VCA

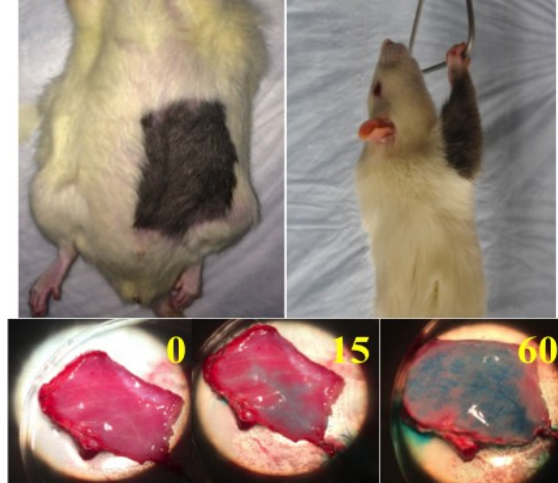


Figure 2.1 Experimental Rat VCA Models. The top left image shows the area where the rat abdominal wall VCA will be harvested from while the top right image shows the rat forelimb VCA model. The bottom three images show an abdominal wall that has been harvested and was perfused with Evans Blue Dye at three different time points.

For this project, adult Lewis rats are used. The bottom three images of **Figure 2.1** demonstrates how the artery that the perfusion needle is connected to is connected to a majority

of the vessels in the tissue and how we are able to pump perfusate to a majority of the abdominal wall.

The rat is first anesthetized with 2.5% isoflurane and the area of interest is shaved and cleaned with alternating applications of betadine and 70% alcohol. Afterwards, the areas of interest are marked. Normally, the abdominal wall removed is approximately 4cm x 4cm in size. The abdominal wall consists of two halves that are separated by the linea alba. An image of the prepared rat can be seen in **Figure 2.2**.



Figure 2.2 Anesthetized Rat with Shaved and Marked Abdomen. The areas of interest are marked with the black lines. The two halves of the abdominal wall are separated by the linea alba. Only one half is used at a time for perfusion or transplantation.

Next, an incision is made to expose the superficial epigastric and femoral vessels. The femoral artery is preserved during the surgery because it is used to perfuse the abdominal wall during surgery as well as for anastomosis during the transplantation surgery. The skin is then cut around the perimeter of marked area and the muscle layer is cut afterwards. During the process of cutting the muscle layers, the edges of the graft are cauterized to prevent excessive bleeding.

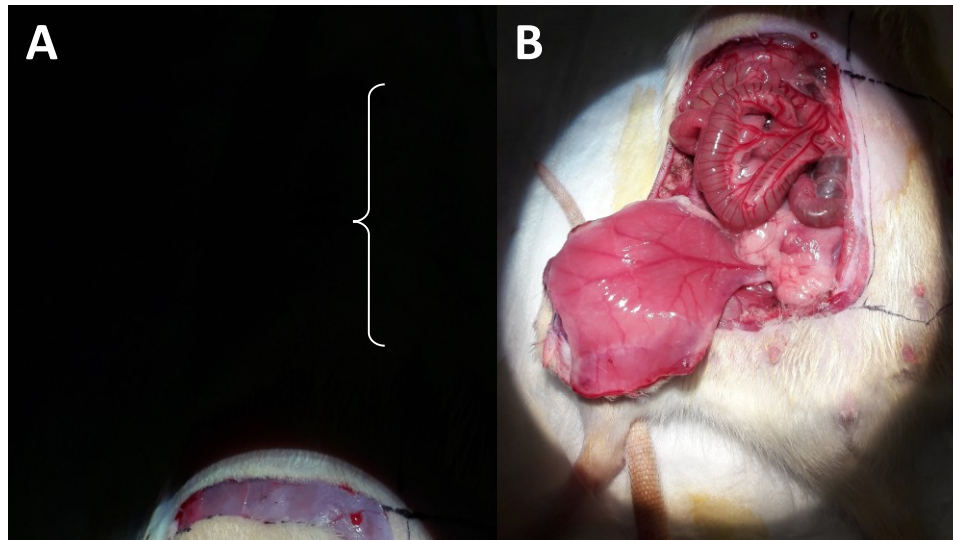


Figure 2.3 The Abdomen with Cut Skin and Cauterized Edges. A shows the cut skin, exposed arteries, and linea alba while B shows the flipped graft with cauterized edges

Afterwards, the external iliac and femoral arteries are dissected and their branches are cauterized. The external ilia is then tied off and the vessels are cut. The blood is flushed out of the graft with 10 mL of heparinized saline (2.4% heparin + 97.6% lactated Ringer's solution). The graft is then covered with wet gauze and prepared for either perfusion or the transplantation surgery if it will not be perfused for preservation. If the graft is to be used for perfusion, the cauterized edges are removed because preliminary perfusion experiments have found that there is an excessive amount of edema due to perfusion. Removal of the cauterized edges allow for the perfusate to leak out of the perfusate, reducing the amount of edema. Afterwards, it is transported into the bioreactor system and a flushing needle is inserted into the femoral artery. **Figure 2.4** shows the graft after the complete harvest surgery.

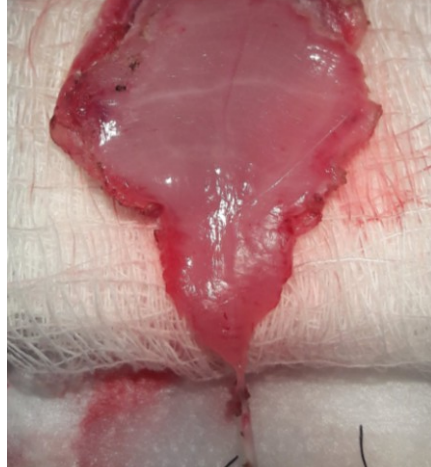


Figure 2.4 The Harvested Abdominal Wall with Intact Vessels.

2.3 Model for Transplantation

To prepare the graft for surgery, the recipient rat will be prepared with similar steps to the donor rat and the femoral vessels are dissected. Edges of the graft are then removed to reduce the size of the transplant and the edges are re-cauterized. The size of the transplant is reduced because larger grafts are unable to be perfused properly from the anastomosis process, leading to necrosis of the tissue. The surgery team discovered the limitation of inadequate perfusion can be achieved by using a smaller graft for transplant. **Figure 2.5** shows a graft with the edges that are marked for removal and the reduced graft.

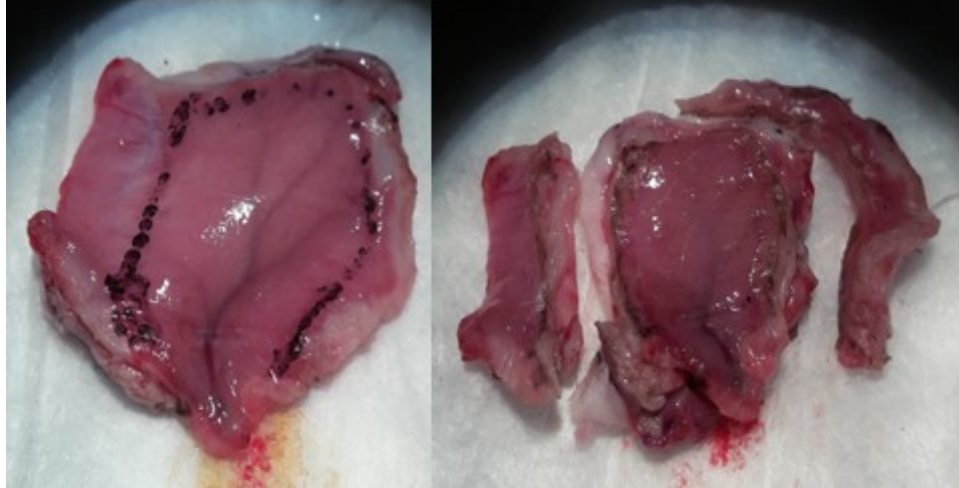


Figure 2.5 The Reduced Graft Sizes. Left: Intact graft with areas marked for removal. Right: The graft with the excess areas removed.

Next, the graft's external iliac vessels are anastomosed to the recipient's femoral muscles. The graft is then placed into the recipient and sutured in place. Later, the recipient rat is then given 0.8 mL of buprenorphine and antibiotics. Afterwards, the surgery site is covered with bandages and the rat is allowed to recover. It is then monitored for several days post-surgery.

Figure 2.6 shows an abdominal wall transplant 5 days post-surgery.



Figure 2.6 A Rat Abdominal Wall Transplant 5 Days Post-Surgery

CHAPTER 3: BIOREACTOR HOUSING AND DESIGN

3.1 Bioreactor Housing Design and Fabrication

The housing provides a sealed and thus safe and sterile environment for the rat VCA. In addition to the sealed environment, the tissue will be coated with a biocompatible electrode gel to 1) enable the conduction of stimulation across the tissue and 2) aid in keeping the tissue hydrated. Below in **Figure 3.1** is an overall SolidWorks view of the proposed bioreactor system. It consists of five main pieces: a base, a left wall, a right wall, a back wall, and a top cover. Each of those pieces will be fabricated from clear polycarbonate, which is a light and durable plastic material that is easy to machine. Since it is clear, it will also allow for visualization of the inner space of the bioreactor once it is sealed. Each of those pieces will be held together with a 0/80 x $\frac{3}{4}$ stainless steel screw. The respective length, width, and height of the bioreactor is 25, 14.6, and 17cm. This allows for the force sensor to be enclosed within the system and for the required tubing, connectors, and perfusion needles to connect between the perfusion inlet and the vessels of the tissue.

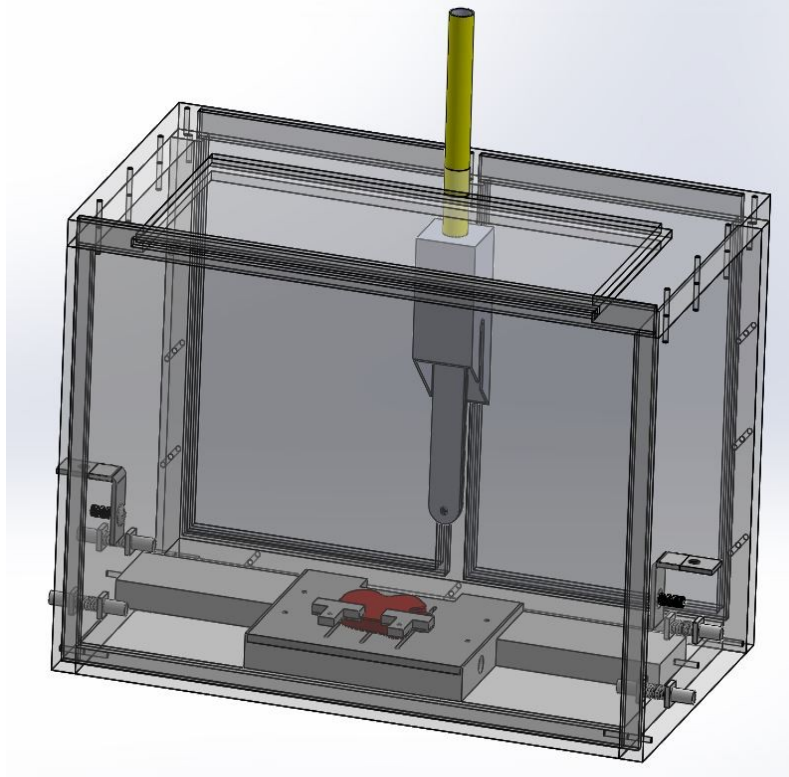


Figure 3.1 Overall Bioreactor Design in Solidworks

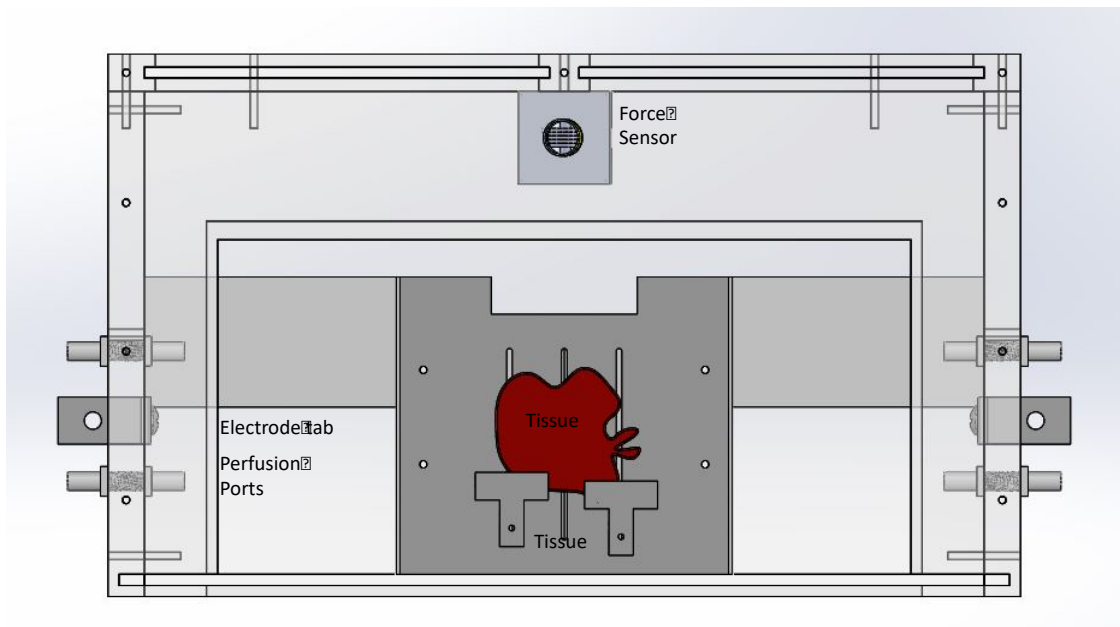


Figure 3.2 Top Down View of Bioreactor. The center red object represents the abdominal wall graft and above it is the force sensor. On both the left and right walls of the bioreactor, there is an inlet and outlet for perfusion as well as a metal bracket tab for the connection of the electrical stimulation system.

The bioreactor includes a platform that the tissue is secured to with two clamps and two sets of perfusion inlets and outlets, which allows for the perfusate to enter and leave the bioreactor. There are two sets of perfusion inlets and outlets because during the abdominal wall harvest surgery, only one half of the abdomen is harvested at a time, thus there are two possible orientations of the grafts and its vessels. This can be seen in **Figure 2.2**. On the left and right walls of the bioreactor, there are two metal brackets that allow for the electrical stimulation signal to conduct from the outside to the inside of the bioreactor. The force transducer, MLT1030/D by ADInstruments, is secured to the back wall via a screw. A thread is used to connect the tissue to the force sensor. These features can be seen in **Figures 3.2 and 3.3**.

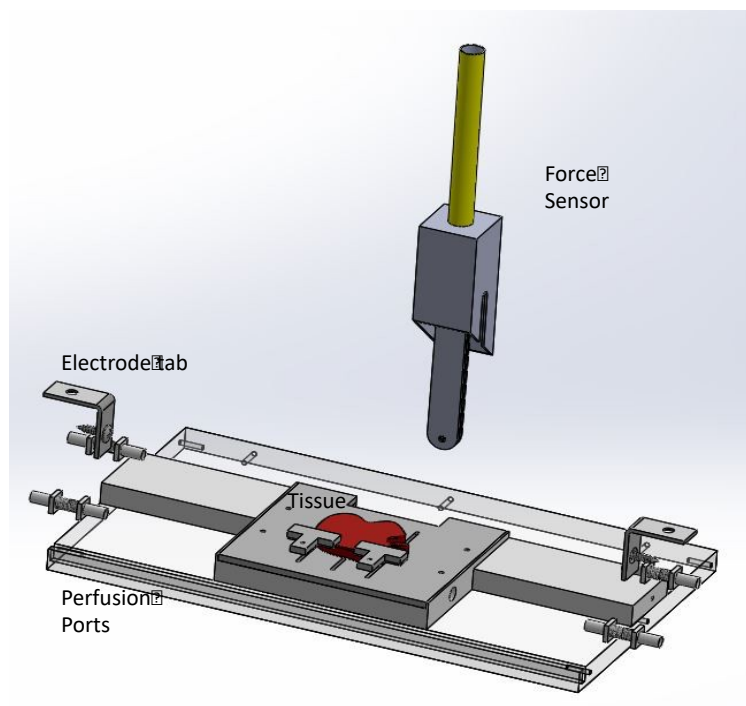


Figure 3.3 Inner Space of Bioreactor. The walls the bioreactor were hidden in order to help visualize the inner components of the bioreactor.



Figure 3.4 The MLT1030/D Force Transducer with the 5 Blades Fanned Out.

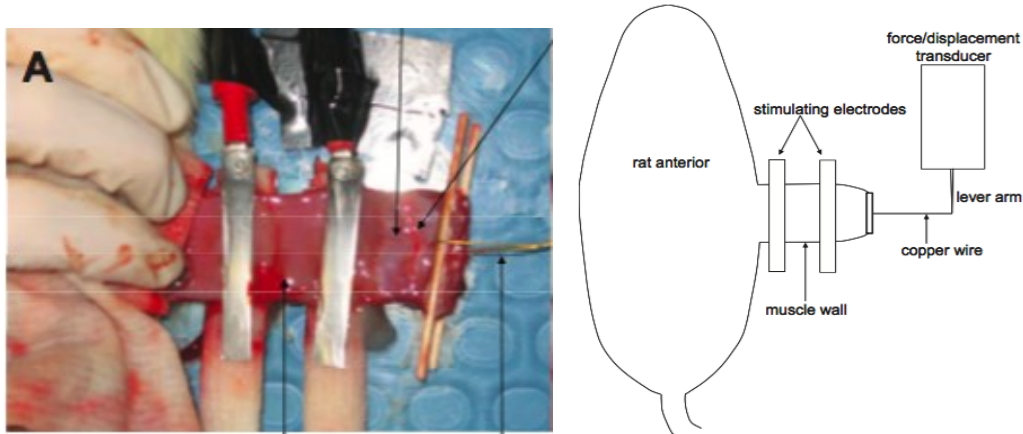


Figure 3.5 The Method of Connecting the Tissue to Force Sensor [44]. Left: A picture of the set up with the flipped abdominal wall, stimulation electrodes, and copper wire. Right: An artistic representation of the same set up.

The MLT1030/D force transducer has five stainless steel blades, four of which are removable in order to adjust the force range and accuracy of the sensor. For preliminary testing, the force transducer will be attached to the abdominal wall via a suture thread, which is similar to the method in a study by Brown *et al* [44]. The following table lists the force ranges and

accuracies of the transducer. This specific force sensor was chosen because it was able read force ranges that are similar to the study by Brown et al, where they isolated and stimulated a rat abdominal wall to measure its force of contraction.

Table 3.1 The Range and Accuracies of the MLT1030/D

| Number of Blades | Range | Accuracy |
|-------------------------|--------------|-----------------|
| 1 Blade | 100mg – 15g | ± 25mg |
| 2 Blades | 6g – 300g | ± 100mg |
| 3 Blades | 10g – 500g | ± 175mg |
| 4 Blades | 15g – 750g | ± 250mg |
| 5 Blades | 20g – 2000g | ± 350mg |

The tissue holder platform has three slits that allow for the clamps to be adjustable. In addition, it allows for the perfusate to collect in a reservoir below the tissue as it drains out from the edges of the tissue during perfusion. The perfusate collects in the reservoir and is able to be pumped out of the reservoir. A close up of the tissue holder platform and the drainage reservoir can be seen in **Figure 3.6**.

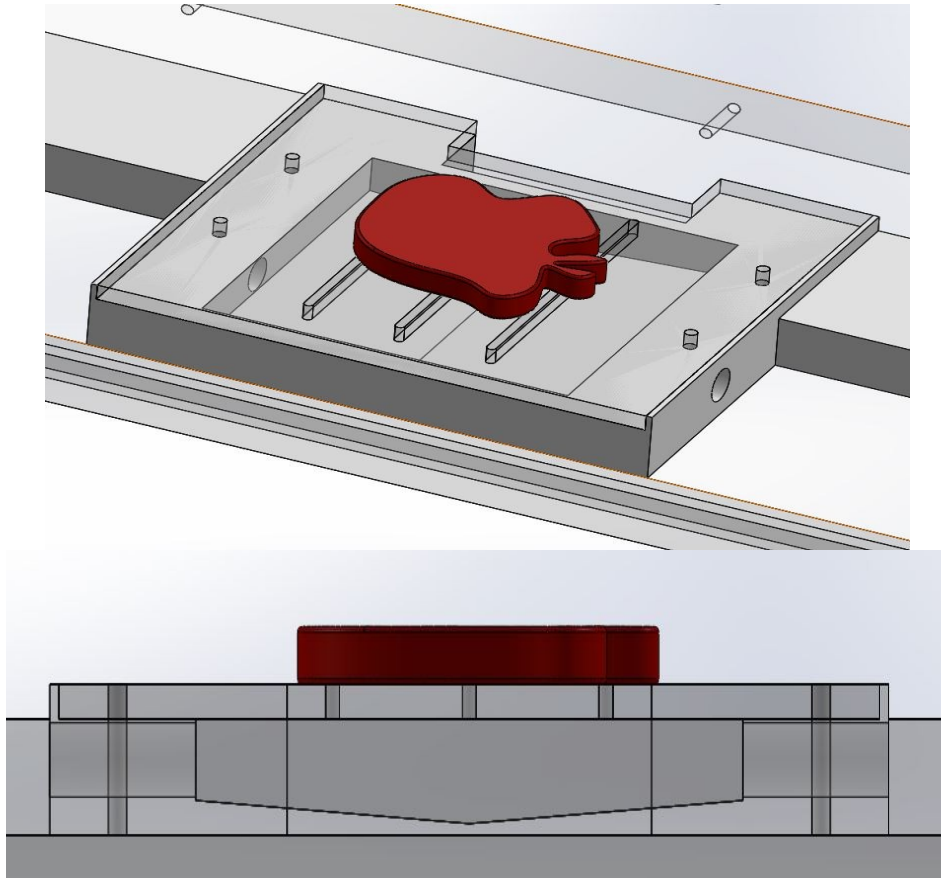


Figure 3.6 Close Ups of the Tissue Holder Platform and Drainage Perfusate Reservoir. As the perfusate drains out of the edges of the graft, it will fall down the slits in the platform (Top) into the perfusate drainage reservoir (Bottom) for collection and pumping back into the main reservoir.

Once the bioreactor is assembled, there are four removable panels that allow access into the bioreactor. This easily allows for the placement of the tissue into the bioreactor and the attachment of the tubing and any other necessary connections. With the panels removed, it allows for access through the front, top, and back of the bioreactor, which is necessary since it can take up to two surgeons to install the graft. These panels can be seen within **Figure 3.7**.

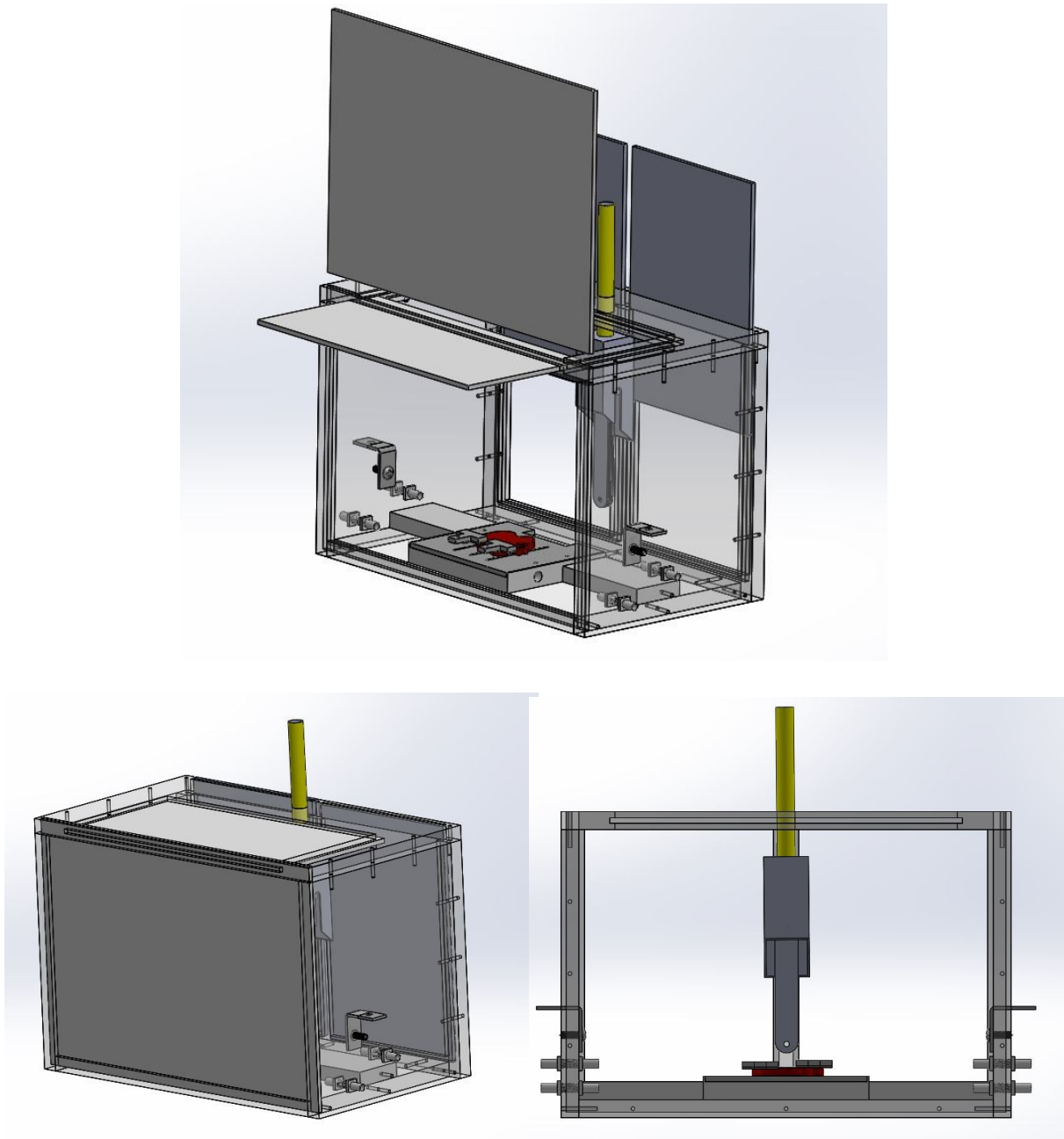


Figure 3.7 The Four Removable Sliding Panels. Top: The four sliding panels are highlighted to show their position in the bioreactor. Bottom Left: The closed bioreactor with panels in place. Bottom Right: The open bioreactor with all sliding panels removed.

3.2 Bioreactor Prototype

As of the time of the writing of this thesis, the finalized bioreactor has not been machined. It will be sent to John Hopkins University's Whiting School of Engineering's Machine Shop for construction. In the meantime, a 3D printed prototype of the bioreactor has

been constructed using the Grayson LabCOTE's LulzBot Taz 5 3D printer and white Acrylonitrile Butadiene Styrene (ABS). It will be used for initial testing and data collection. Below are several images of the 3D printed bioreactor that was used for testing.



Figure 3.8 Side Views of Closed 3D Printed Bioreactor Prototype



Figure 3.9 Close Up of Perfusion Ports and Electrode Tab

The ports were changed from the original design and tubing was pushed through the walls instead of using barbed plastic tube fittings. This was changed due a leaking problem. The metal L bracket is used to connect the electrical stimulation system to the bioreactor via an alligator clip.

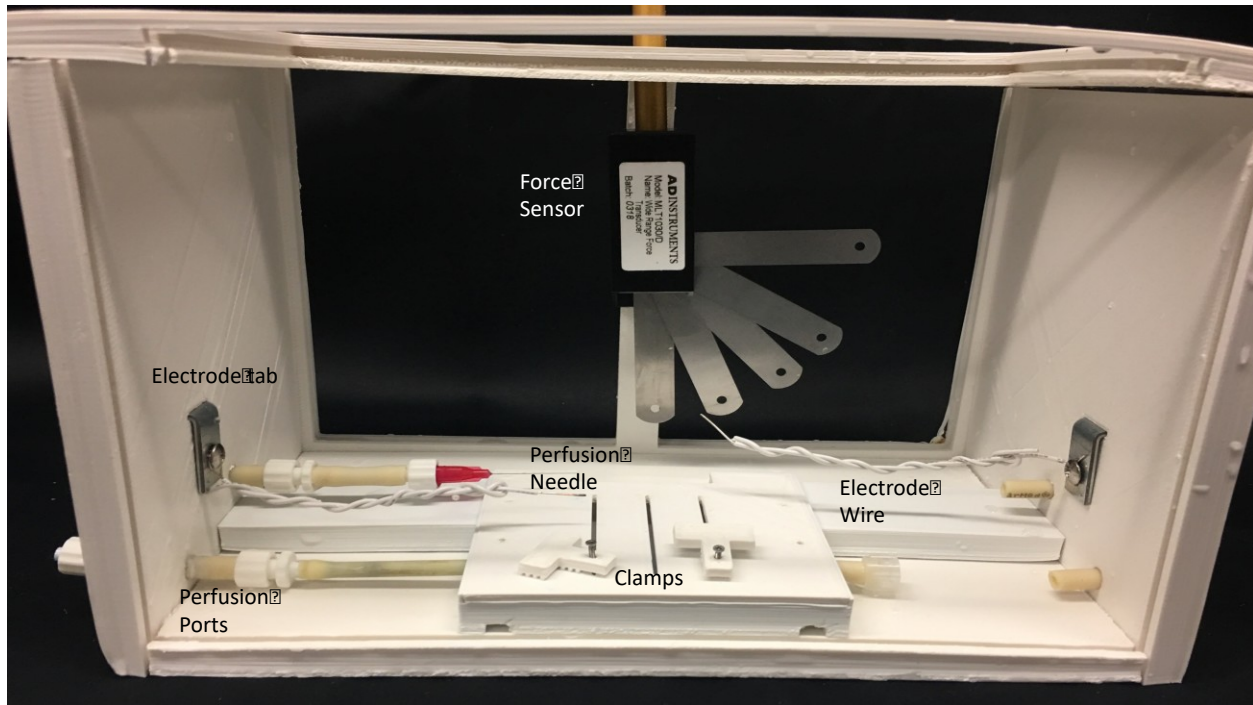


Figure 3.10 Front View of Opened 3D Printed Bioreactor Prototype. The inner components can be seen: the fanned out force sensor, perfusion tubing and needle, electrode wires, and clamps.

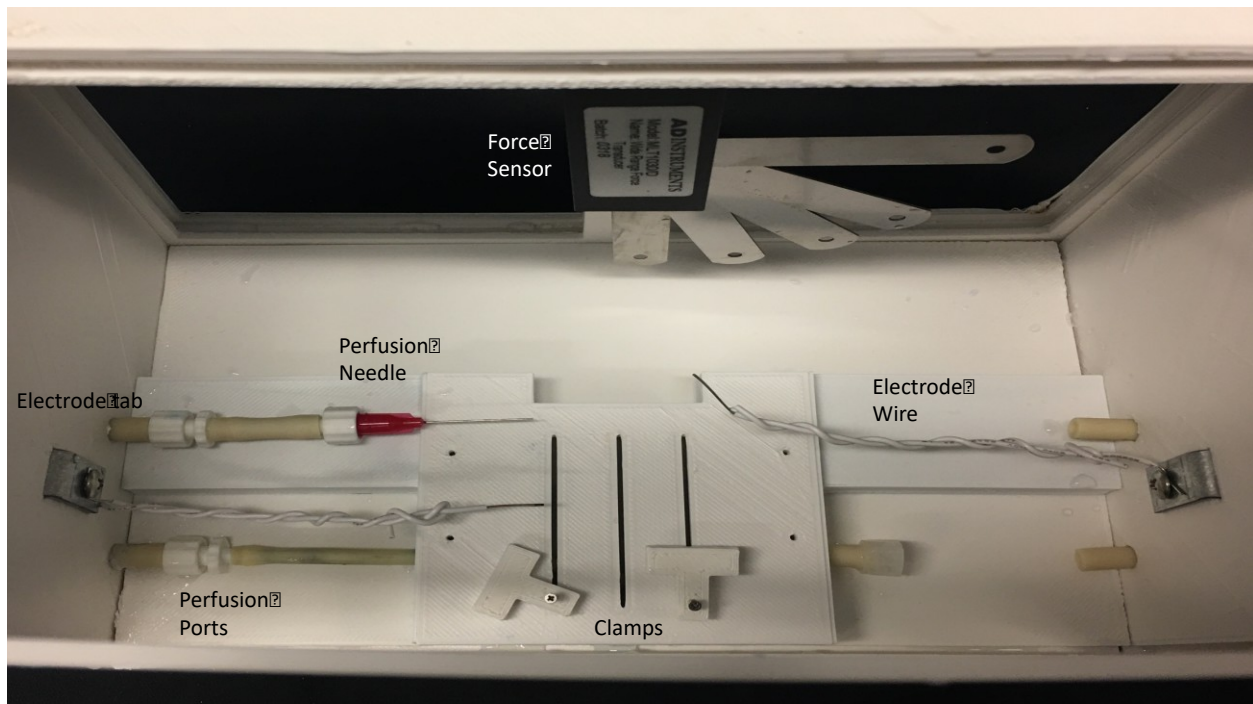


Figure 3.11 Top Down View of Opened 3D Printed Bioreactor Prototype

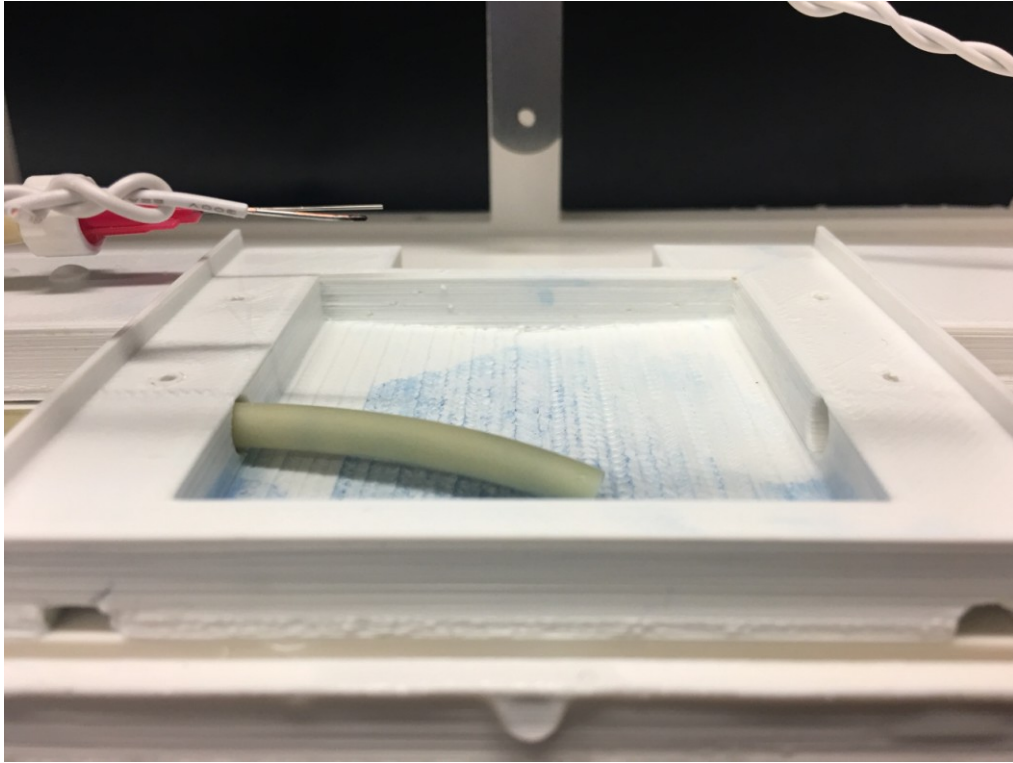


Figure 3.12 Close Up of Perfusate Drainage Well. The holder platform has been removed to allow visualization of the lower well.

3.3 Sterile Assembly

In order to ensure sterility of the bioreactor, it has been designed to be able to break down into multiple pieces for sterilization. An exploded view of the bioreactor and its parts can be seen in **Figure 3.13**. After the individual pieces are cleaned and sterilized with 70% ethylene oxide, the bioreactor parts are assembled together and sealed within a sterile environment such as a clean room. Afterwards, the bioreactor is transported to the surgery site and opened to allow the installation of the graft. Even though the surgical field is considered sterile, there is a minimal chance of contamination during the process of the graft installation inside the bioreactor. Therefore, antibiotics should be included within the perfusate to further minimize any risk of infection.

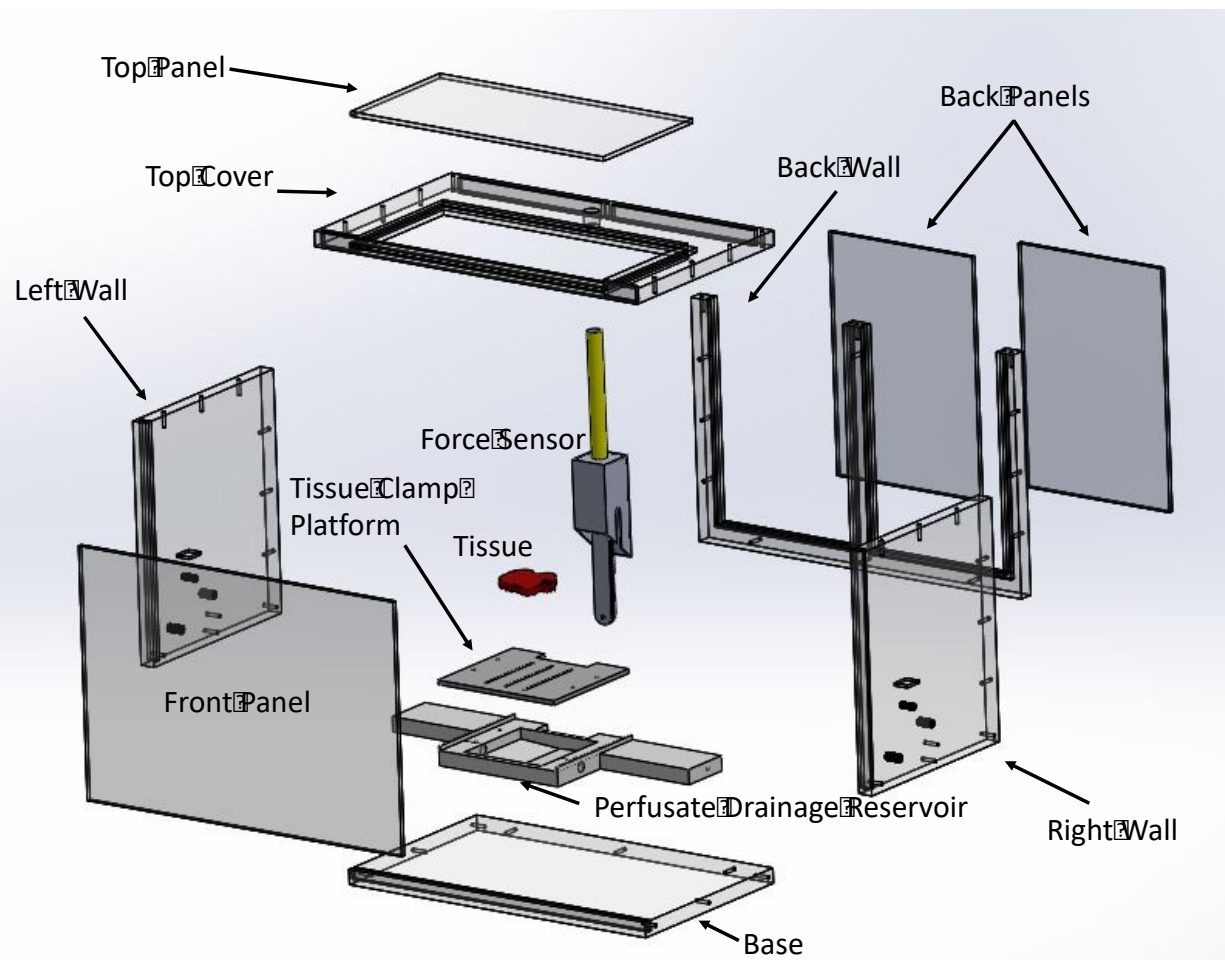


Figure 3.13 Exploded View of Bioreactor

CHAPTER 4: PERFUSION TESTS

4.1 Flow Through System

In order to maintain the graft at a functioning state outside of the body, an adequate supply of oxygen and glucose is needed to be delivered throughout the graft. Thus a peristaltic pump will be used to drive the perfusate throughout the system while the other components of the flow circuit will condition the media as well as monitor various components of the perfusate. In this iteration of the flow circuit, a heater and bubble trap were not included. A hot plate will be used to heat the entire perfusate instead. The needle used to perfuse the tissue is a 25-gauge needle with a 1-inch tip by Nordson EFD.

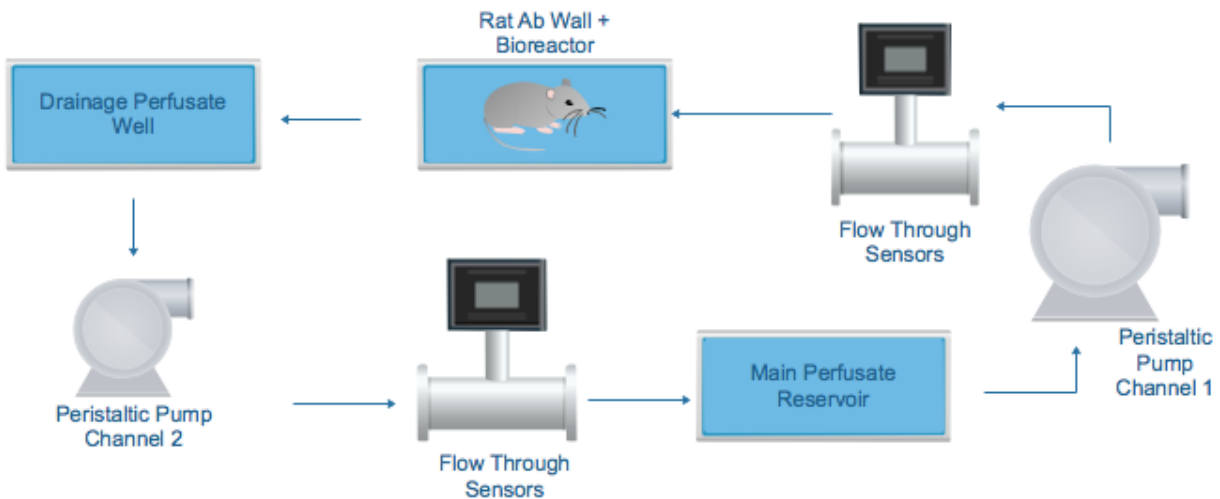


Figure 4.1 Flow Circuit Diagram. Perfusion starts with the peristaltic pump pulling perfusate from the main reservoir and driving it through the series of inline sensors and into the bioreactor with the abdominal wall. From there, the perfusate drains out of the edges of the graft and into the drainage well. From there, the perfusate is pulled into the second series of inline sensors and back into the main perfusate reservoir

4.1.1 Components of Flow Circuit

This system uses 1/8-inch inner diameter PharMed BPT biocompatible tubing to connect the individual parts of the flow system. The Ismatec IP8 is an 8 channel peristaltic pump whose speed can be controlled. It also has an analog interface on its back to allow for electronic control

of the pump. This allows for the pump to be automated. A custom MATLAB graphic user interface and script to control that interface were created. It allows for the user to control the on and off cycle of the pump for intermittent perfusion is desired. The code for the interface and script can be found in the appendix.



Figure 4.2 The Ismatec IP 8 Peristaltic Pump

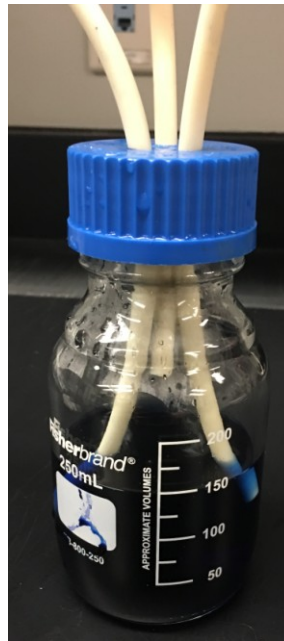


Figure 4.3 Main Perfusate Reservoir with a Mix of Evans Blue Dye and Saline. It was machined from a 250mL glass media bottle with three holes drilled in the cap. One for pump to pull perfusate out, one for pumping perfusate back in, and one for passive oxygen diffusion into the perfusate.

Originally, an oxygenator was to be added into the perfusion circuit. However, calculations were performed to determine the amount of oxygen needed by the rat abdominal

wall and it was found that passive oxygen diffusion provided an adequate amount of oxygen. Thus an additional opening to the reservoir was added. A tube with a bacterial filter would be inserted into that hole. This allows for passive oxygen diffusion while maintaining the sterility of the perfusate. Below are calculations for passive oxygen diffusion and estimating the rate of oxygen consumption for the rat abdominal wall.

Rate of Oxygen Consumption: $600 \text{ uL/hr/g} = 10 \text{ uL/min/g}$ [45]

Rate of Oxygen Consumption Per Gram: $10 \text{ uL/min/g} * (1\text{mol}/22.4\text{L}) = 4.46\text{E-}7 \text{ mol/min/g}$

Average Weight of Rat Abdominal Wall = 5g

Rate of Oxygen Consumption = $2.23\text{E-}6 \text{ mol/min}$

P_{O_2} : atmospheric partial pressure of O_2 : 0.21 atm

H: Henry's constant: $769.23 \text{ [(L * atm) / mol]}$

C_{O_2} : concentration of O_2 in perfusate

$$P_{O_2} = H * C_{O_2}$$

$$C_{O_2} = P_{O_2} / H = 0.21 \text{ atm} / (769.23 \text{ (L * atm)/mol})$$

$$C_{O_2} = 2.73\text{E-}4 \text{ mol/L}$$

Currently use 80 mL of perfusate at a time:

$$O_2 = C_{O_2} * L = 2.73\text{E-}4 \text{ mol/L} * 0.08\text{L} = 2.18\text{E-}5 \text{ mol of } O_2$$

To measure the composition of the perfusate, various inline sensors will be incorporated into the perfusion loop. Included are one pressure transducer, two oxygen probes, 2 thermocouples, and 2 pH probes. The ion sensors are fitted with a flow through fitting as seen in **Figure 4.5**. The sensors are all connected to the 16/35 PowerLab by ADInstruments, which is a data acquisition unit that is capable of reading up to 16 inputs at once. The LabChart program is used to read the data from the PowerLab.



Figure 4.4 An Ion Sensor with a Flow Through Fitting

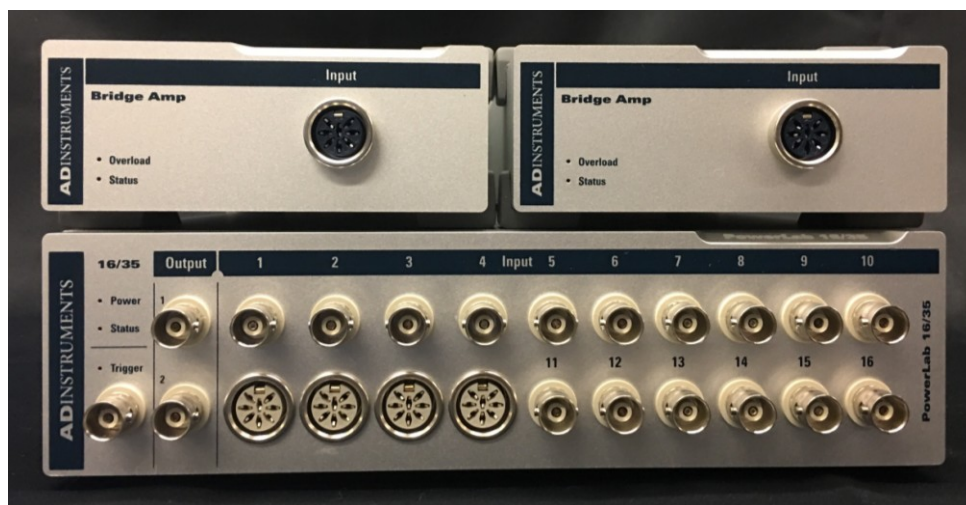


Figure 4.5 The PowerLab with Two Accompanying Bridge Amplifiers

4.1.2 Calibration of the Sensors

Due to the nature of the bioreactor and the perfusate drainage method, the pressure sensor is only able to be used at the inlet while the temperature, oxygen, and pH sensors can be used to analyze the perfusate as it enters and leaves the bioreactor.

All of the sensors were connected inline and different solutions were pumped through them in order to calibrate the sensors and ensure that the readings were accurate. This can be seen in a screenshot of the LabChart program in **Figure 4.7**. All of the data can be exported into various file formats for further data processing. Initially, the circuit was primed with standard cold tap water. This can be seen with the vertical dotted line labeled prime. At time zero, the source of the pump inlet was switched to a beaker full of hot tap water. The temperature readings of the temperature sensors, T_1 and T_2 , can be seen rising up to almost 35°C. At 1:00, the source was switched to a beaker full of cold tap water and the temperature readings can be seen dropping down to about 21°C. At 2:00, the source was switched to a 0% oxygen solution (made by adding 12g of sodium metabisulfite to 500mL of water). At about 2:30, the oxygen readings

can be seen dropping down 0%. The pH readings also drop down to about 2 because the 0% oxygen solution is acidic. At 3:00 and 4:30, the source was switched to a beaker full of a 4.01 and 7.01 pH buffered solution respectively. About 30 seconds after those respective time points, the pH readings can be seen rising to 4 and 7. The force sensor was connected but was not used during this test. The pressure sensor was also attached but a perfusion needle was not attached to the end of the tubing so pressure remained around 15mmHg. The pump was operated at 100% of its max speed during the majority of this test. The pump ran at 5% of its max speed during brief periods of switching the reservoir and between 4:00-4:30.

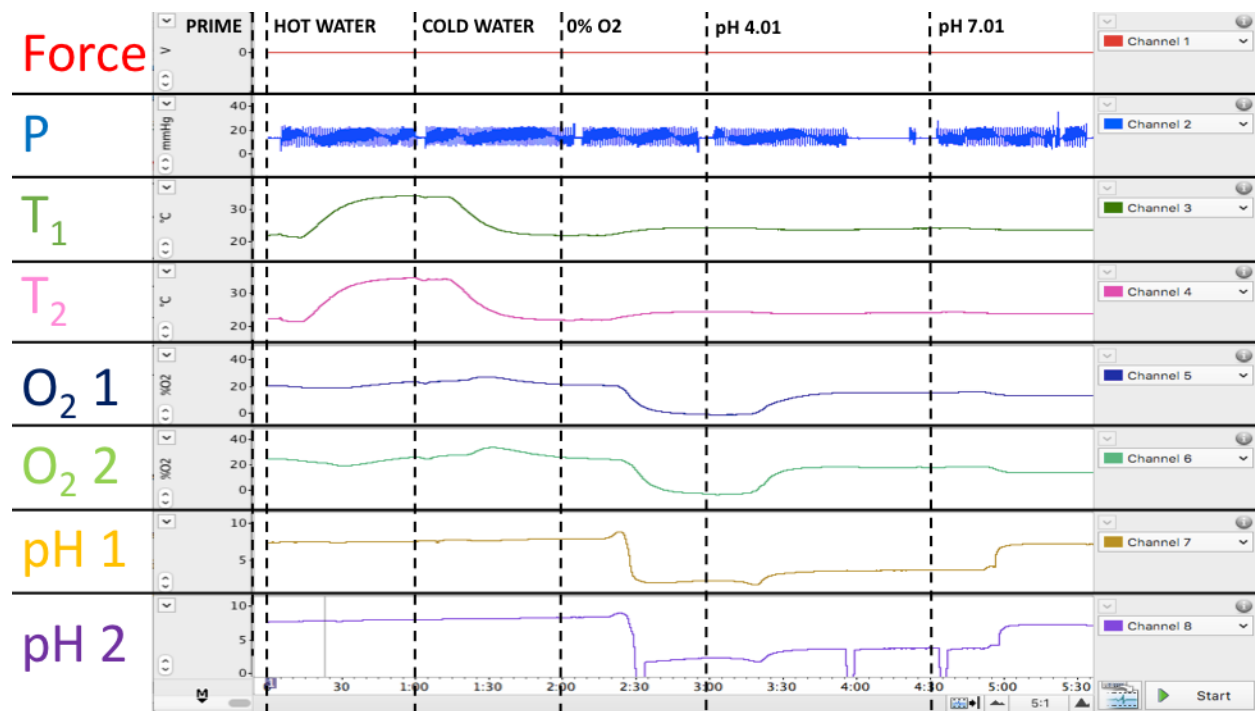


Figure 4.6 Flow Through Sensor Graph Readings from LabChart. The vertical dashed lines represent when the perfusate was changed. At first, the system was primed with standard tap water (PRIME). At time zero (0:00), the source was changed to hot tap water. At 1:00, the source was changed to cold tap water. At 2:00, the source was changed to a 0% oxygen solution. At 3:00 and 4:30, the source was changed to a 4.01 pH buffer solution and 7.01 pH buffer solution respectively.

4.2 Experimental Set Up and Methods

The bioreactor prototype was tested with an abdominal wall as a proof of concept. The abdominal wall was harvested according to the steps in **Section 2.2** with the exception that the

vessels were not cut until the bioreactor system was set up. Thus, the abdominal wall had its edges cauterized but was not cut off from the blood supply for about 2 hours. Once the bioreactor was set up, the vessels of the graft were cut and the 25-Gauge perfusion needle was inserted into the artery. The blood was then flushed out of the graft with heparinized saline as described in **Section 2.2**. Next, the tissue was clamped within the bioreactor and a suture wire was threaded through the tissue and tied to the end of the force sensor. **Figure 4.7** shows how the tissue was installed within the bioreactor. The rest of the perfusion system was connected to the tissue and heparinized saline was pumped throughout the system and graft at 0.5 mL/s to allow for an electrical stimulation test as described in **Section 5.3.2**. The complete perfusion system can be seen in **Figure 4.8**.

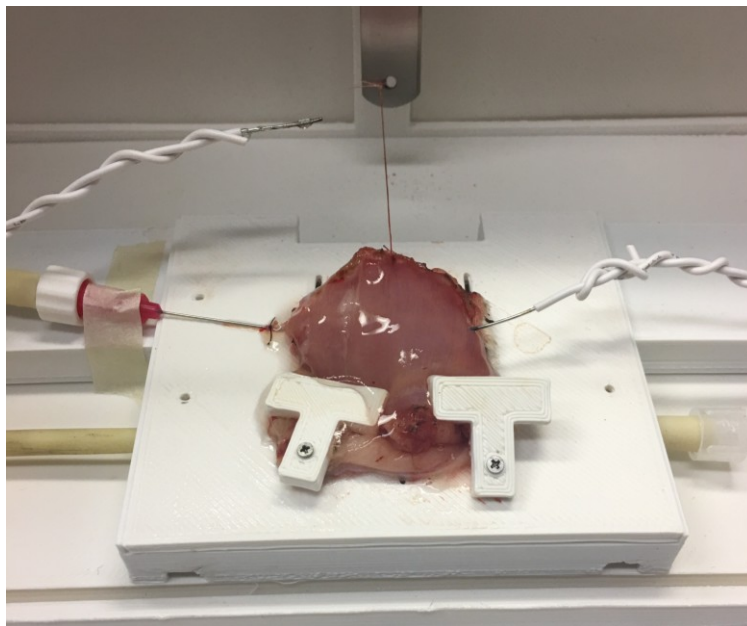


Figure 4.7 How the Tissue is Attached to the Force Sensor

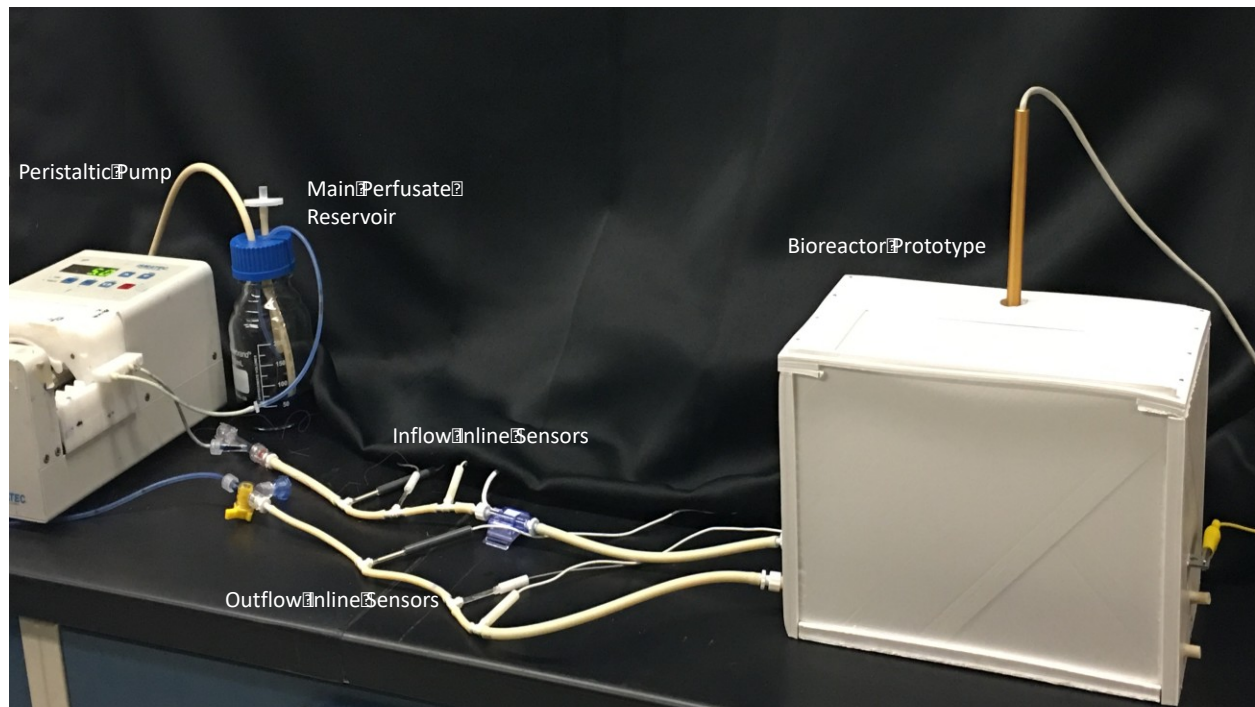


Figure 4.8 The Perfusion System Connected to the Bioreactor Prototype. On the right is the bioreactor prototype with force sensor protruding from its top. To its left are the inline sensors, the peristaltic pump, and the main perfusate reservoir.

After the stimulation test was completed, Evans Blue Dye was perfused throughout the system as a proof of concept of the perfusion system. The blue dye allows for the visualization of the perfusate as it travels through the graft. During all of this, the flow through sensor system was connected to the bioreactor in order to take force, pressure, temperature, oxygen, and pH readings.

4.3 Results

Heparinized saline was perfused through the abdominal wall for one hour at a flow rate of 0.5 mL/s. Afterwards, Evans Blue Dye was perfused through and the tissue was rapidly colored by the tissue. Images of the tissue progressively becoming more dyed can be seen in **Figure 4.10**.

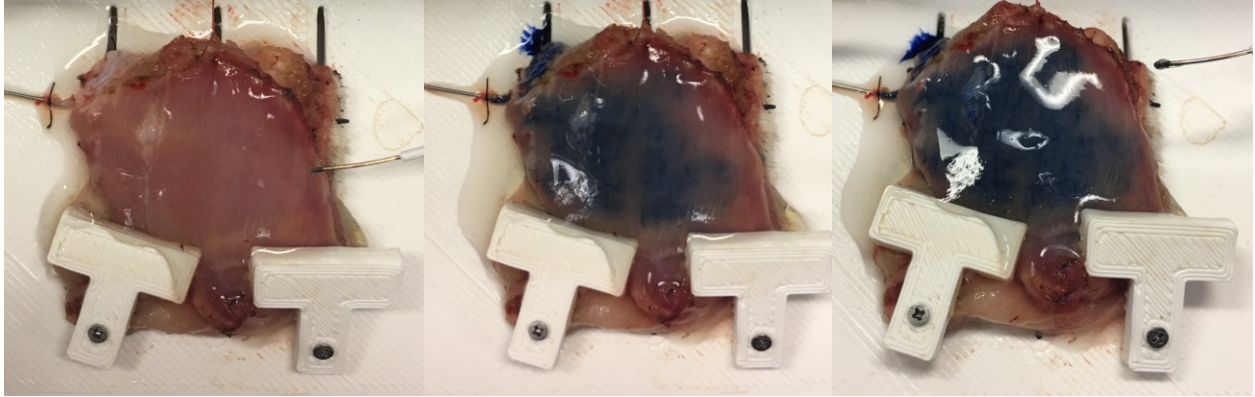


Figure 4.9 Perfusion of the Abdominal Wall with Evans Blue Dye at Three Different Time Points

Below are several graphs of the sensor readings throughout the perfusion period.

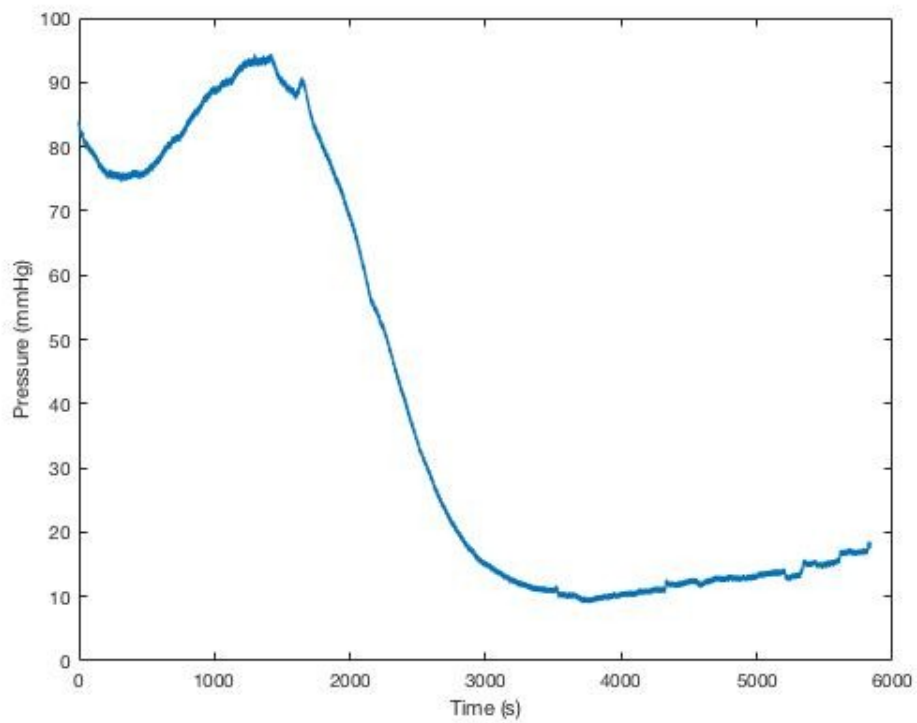


Figure 4.10 Pressure Readings

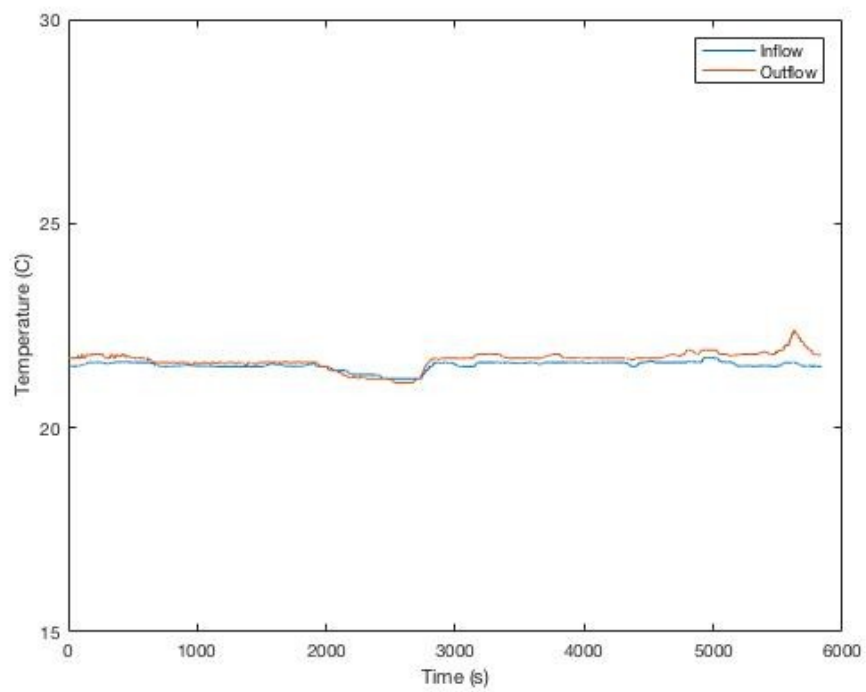


Figure 4.11 Temperature Readings

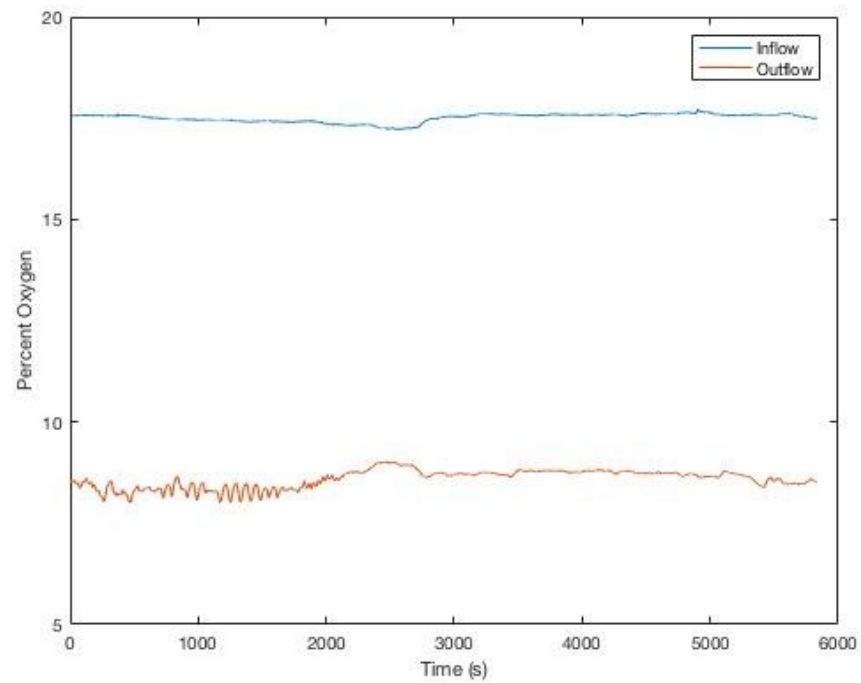


Figure 4.12 Percent Oxygen Readings

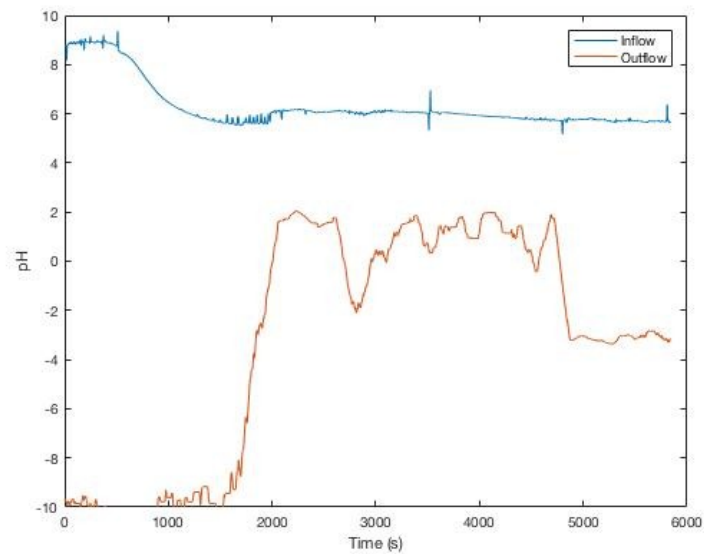


Figure 4.13 Percent pH Readings

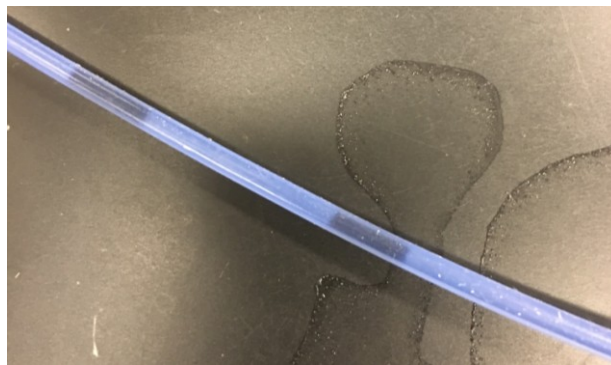


Figure 4.14 Air Bubbles in the Outflow Tubing



Figure 4.15 Perfusate Reservoir with Mixed Saline. Normally saline is clear but the saline is colored pink after haven been driven through the abdominal wall.

4.4 Discussion

The goal of this section was to develop a perfusion system that is capable of delivering perfusate throughout the tissue while conditioning the perfusate. As the perfusate is driven though the vessels of the abdominal wall, oxygen and other nutrients are delivered to enable

aerobic metabolism. **Figure 4.16** shows the perfusate reservoir with saline, which is normally clear. The pink coloration shows how the perfusion circuit is able to operate within a continuous loop: perfusate is pulled from the reservoir and pumped throughout the bioreactor and tissue until it leaks out and is pumped back into the reservoir.

As seen in **Figure 4.9**, the pump is able to connect into the bioreactor to perfuse the abdominal wall. As Evans Blue Dye is pumped throughout the circuit, the abdominal wall is colored blue. **Figure 4.3** shows a picture of the main reservoir that is full of saline. The blue coloration is due to the blue dye that was collected as it leaked out of the tissue.

Figures 4.11-4.14 show the pressure, temperature, oxygen, and pH readings of the perfusate during the perfusion. The pressure graph shows an initially high pressure reading of about 90 mmHg before dropping down to about 10 mmHg while the temperature graph shows that the temperature of the perfusate as it enters and leaves the bioreactor is about 22°C, which is expected as the hot plate was not used. The oxygen graph shows a higher concentration of oxygen in the perfusate as it enters the bioreactor (about 17%) compared to the perfusate as it leaves the bioreactor (about 8%). This is somewhat as expected because the abdominal wall should use some oxygen for metabolism. However, the 9% difference is significantly greater than expected. The pH of the perfusate readings indicate that the system stabilizes around a pH of 6 as it enters the bioreactor and around 2 as it leaves. This is also somewhat expected since the abdominal wall is expected to be undergoing ischemia, but there is a drastic difference in the pH levels. In addition to the strange values, there are many fluctuations in the sensors, which is related to their sensitivity. Thus, the sensors should be placed in a secure location during their readings in order to prevent the noise. As expected, there are air bubbles in the outflow tubing returning to the main reservoir, as seen in **Figure 4.15**, which would affect the outflow readings.

This is due to the nature of the bioreactor and how the perfusate drains into a pool before being pumped back into the main reservoir. A bubble trap should be placed between the outflow port of the bioreactor and the sensors to fix this problem in the future. In addition, all of the data has been smoothed using a moving average function.

Overall, the bioreactor allows for the perfusion of the abdominal wall while the inline sensors are able to measure the components of the perfusate. However, the readings from the sensors are unstable and further work needs to be done to stabilize them.

CHAPTER 5: ELECTRICAL STIMULATION

5.1 Electrical Stimulation Background

Several studies have shown that electrical stimulation can help with wound healing, muscle growth, nerve regeneration, and as well as reducing muscle atrophy after injury [46-49]. By combining electrical stimulation of the graft along with normothermic perfusion, we hope to both enhance and extend the preservation time of the rat abdominal wall VCA model.

Monophasic stimulation only has one polarity, such as using direct current, and results in a net ion flow in tissue, which can cause tissue damage and corrosion [50]. Those disadvantages can be avoided with Biphasic stimulation with alternating current.

5.2 Circuit Design and Theory

The circuit used for electrical stimulation is an H-Bridge Circuit. It allows for the voltage applied across a load to reverse its polarity. In other words, the H-Bridge Circuit converts direct current to alternating current, which allows for biphasic stimulation of tissue. An H-Bridge circuit is essentially a series of four switches or gates that open and close to adjust the polarity of the voltage that is applied across a load. This H-Bridge Circuit uses two P-Channel MOSFETs and two N-Channel MOSFETs as the four switches.

A MOSFET (metal-oxide-semiconductor field-effect transistor) is a type of transistor that changes its conductance between its Source and Drain terminals based on the voltage applied at one of its terminals, the Gate. P-Channel MOSFETs are open by default and only close when a positive voltage is applied at its gate. N-Channel MOSFETs are closed by default and only open when a positive voltage is applied at its gate. A schematic for the P-Channel and N-Channel MOSFETs can be seen in **Figure 5.1**.

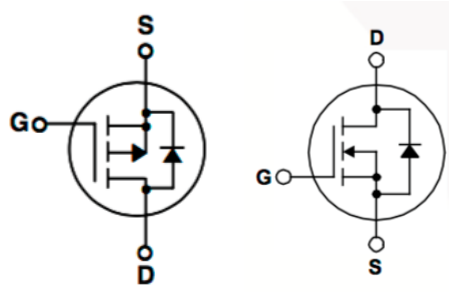


Figure 5.1 Schematics of P-Channel and N-Channel MOSFETs

The four MOSFETs are controlled by two inputs voltages, Inputs A and B, which are determined by the Arduino Microcontroller output pins. Between the Inputs and the MOSFETs are two NPN transistors and two current limiting resistors. The transistors protect the output pins from the high voltage running through the circuit by only allowing current to flow from the output pin into the rest of the circuit instead of vice versa. The current limiting resistors simply limit the amount of current that comes from the output pins of the Arduino Microcontroller to protect the transistors. Throughout the rest of the circuit, there are several gate bleeding resistors, which allow the MOSFETs to drain properly and thus function properly. **Figure 5.2** shows a schematic of the H-Bridge circuit and all of its components. The load in the center of the circuit is where the polarity of the voltage switches and thus that is where the tissue will be connected to the circuit. In other words, the tissue that is to be stimulated is the load.

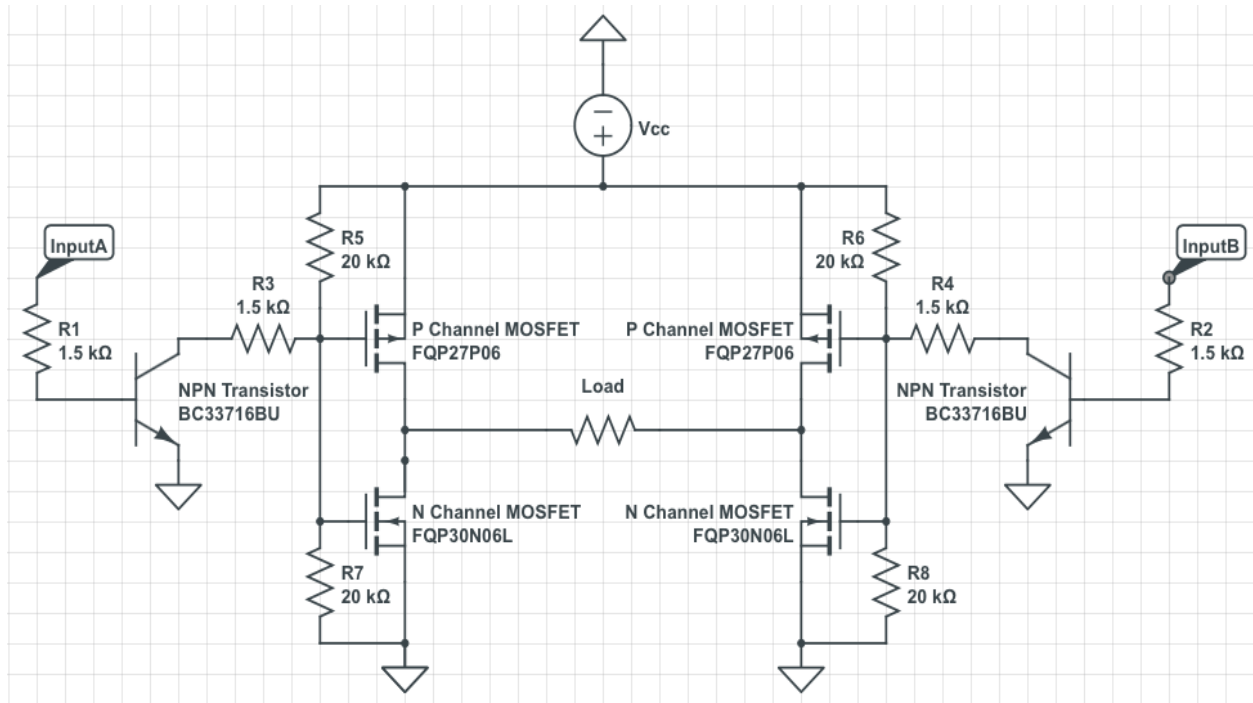


Figure 5.2 H-Bridge Circuit Schematic. This includes the power source (V_{cc}), the 4 MOSFETs that act as gates, the load that the current passes through for stimulation, and the two inputs A and B.

The orientation of the four MOSFETs changes based on the voltages from the two Inputs. **Figure 5.4** shows the type of waveform produced by flipping the inputs, a biphasic or alternating waveform as measured by an oscilloscope. By having the microcontroller turn on and off the Inputs at an appropriate rate, any desired frequency for stimulation can be produced.

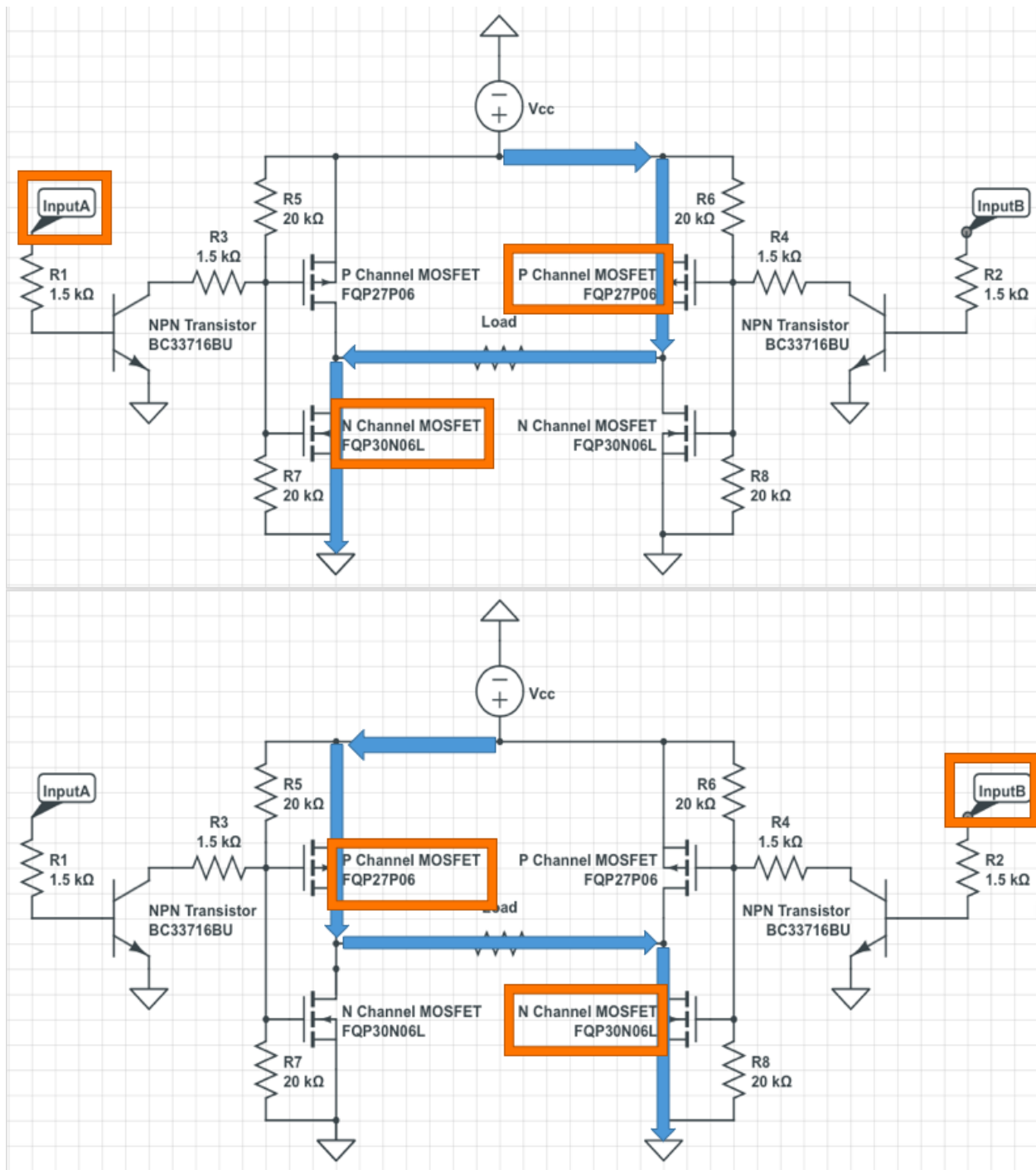


Figure 5.3 The Two Possible Orientations of the H-Bridge Circuit. In the top image, Input A is turned on while Input B is off. This allows for the top right P Channel MOSFET and the bottom left N Channel MOSFET to open, allowing the current to flow from the right to left across the load. The bottom image shows the circuit's activity when Input B is turned on while Input A is off. In this case, the orientation of the open gates allows for the current to flow from left to right across the load.

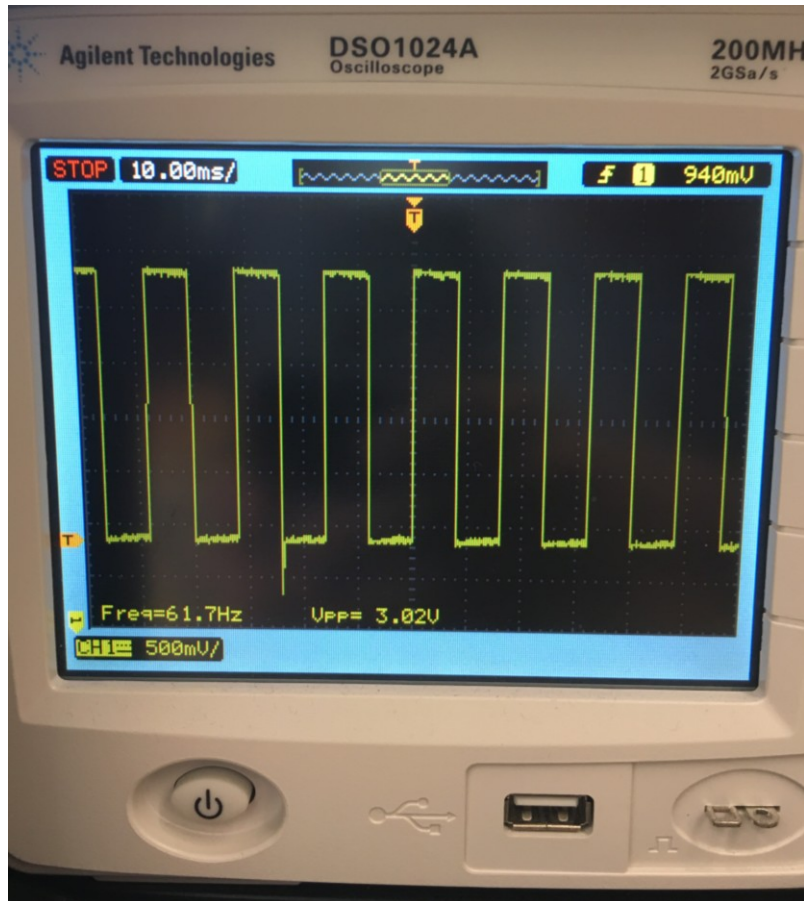


Figure 5.4 The Output Waveform from the H-Bridge Circuit Measured by an Oscilloscope.

5.3 Experimental Set Up and Methods

Two separate sets of experiments were done with the electrical stimulation system. The first was an isolated test of the electrical stimulation system on a harvested rat abdominal wall as a proof of concept. The second was a test of the electrical stimulation system in conjunction with the complete bioreactor system and perfusion test from Chapter 4.

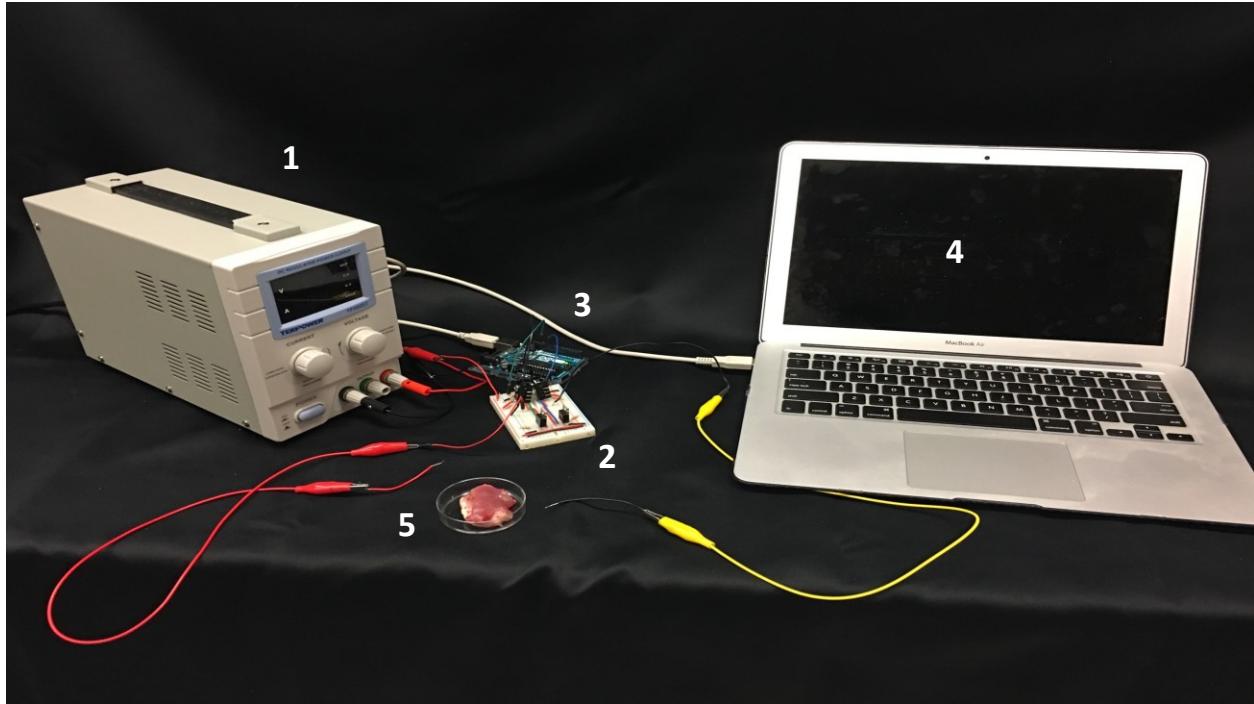


Figure 5.5 Electrical Stimulation Set Up. 1) A power supply to provide the stimulus, 2) an H-Bridge Circuit to direct the stimulus, 3) an Arduino Microcontroller to control the gates of the H-Bridge Circuit, 4) a laptop that powers the Arduino Microcontroller and uploads code into the microcontroller, and 5) a pair of stimulation electrodes.

5.3.1 Electrical Stimulation Experiment 1: Proof of Concept

The rat abdominal wall was harvested according to the steps from Chapter 2 with the exception that the vessels were not dissected. This was done in order to speed up the surgery because the experiment did not involve perfusion so perfusion and preservation of the blood vessels were not necessary. The surgery was completed at 10:54 A.M. and the electrical stimulation tests began at 11:04 A.M. Before stimulation, the tissue was placed in a small petri dish and coated with a thin layer of Signa Gel Electrode Gel. Afterwards, two tin coated 22-gauge copper wires were connected between the H-Bridge circuit's output and the gel. An iPhone 6S Plus was mounted above the tissue in order to record the stimulation results since the force sensor was not available for use at the time. The tissue was then stimulated with 7 V at 70 Hz with 300 ms pulse trains every 4.7 seconds. Afterwards, the video was processed inside

MATLAB in order to measure the percent of contraction of the tissue upon stimulation. The script analyzed each frame of the video by cropping everything that was not within the area of interest (the tissue itself), converting the frame to gray scale, thresholding the image, and then measuring the white area or the area of the tissue. After measuring the area of interest for each frame, the script would look for the large and lowest areas of tissue calculated. Those would represent the tissue at an unstimulated and stimulated state. The script would then use two numbers to calculate the percentage of area contraction with the following equation:

$$\text{Percentage of Area of Contraction} = \frac{(\text{Max Area} - \text{Min Area})}{\text{Max Area}} * 100$$

5.3.2 Electrical Stimulation Experiment 2: Within the Bioreactor

The abdominal wall used for this experiment is the same wall used in **Section 4.2**. The abdominal wall was removed from the rat and its edges were cauterized but the vessels were still connected as the bioreactor system required time to set up. This took about 2 hours. Once the bioreactor was ready for the abdominal wall, the vessels were cut and the perfusion needle was then inserted into the vessels to flush out the blood with heparinized saline. Next, it was clamped down within the bioreactor and connected to the force sensor via a suture thread. The electrode gel was then applied to the top surface of the abdominal wall and the electrode wires were placed to contact the gel. Heparinized saline was then pumped throughout the tissue at 0.5 mL/min throughout the experiment. 7V of stimulation were applied at 70 Hz to the tissue in 300 ms pulse trains every 4.7 seconds and the force of contraction was measured. The same phone was used to record a video of the tissue contraction.

5.4 Results

5.4.1 Electrical Stimulation Experiment 1 Results

Figure 5.6 shows two frames taken from the recorded video in **Section 5.3.1**. The left image shows the tissue when it is unstimulated while the right image shows the tissue contracting due to stimulation. **Figure 5.7** shows the different stages of the video processing as described in **Section 5.3.1**. According to the script, the electrical stimulation caused a 14.5% change in area upon stimulation.

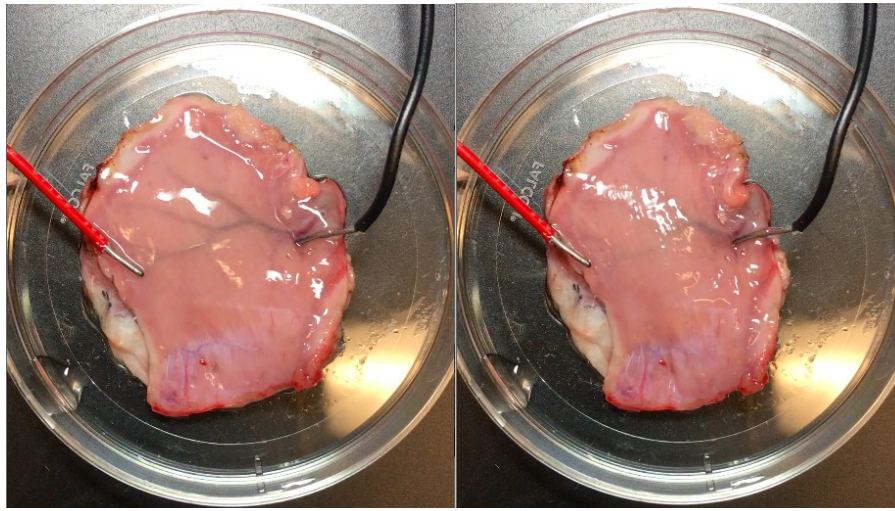


Figure 5.6 Experiment 1: Frames of the Tissue when Unstimulated (Left) and Stimulated (Right)

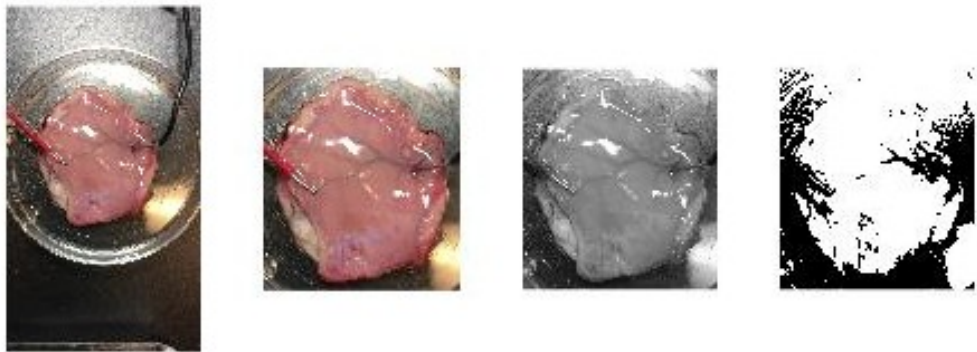


Figure 5.7 Different Stages of the Video Analyzing Process. 1st: Entire Frame, 2nd: Cropped Frame, 3rd: Grayscale, and 4th: Threshold Images

5.4.2 Electrical Stimulation Experiment 2 Results

Figure 5.8 shows two frames from a video recording of the tissue being stimulated within the bioreactor. Since there was very little contraction, an arrow and line were placed at the same position in both frames to help visualize the contraction. On the right image, the tissue is contracted from stimulation and there is a greater distance between the line and the tissue compared to the left image where the tissue is not stimulated. In addition, the pattern of light reflection due to the electrode gel is different in both images, which suggests that the tissue contracted and changed shape.

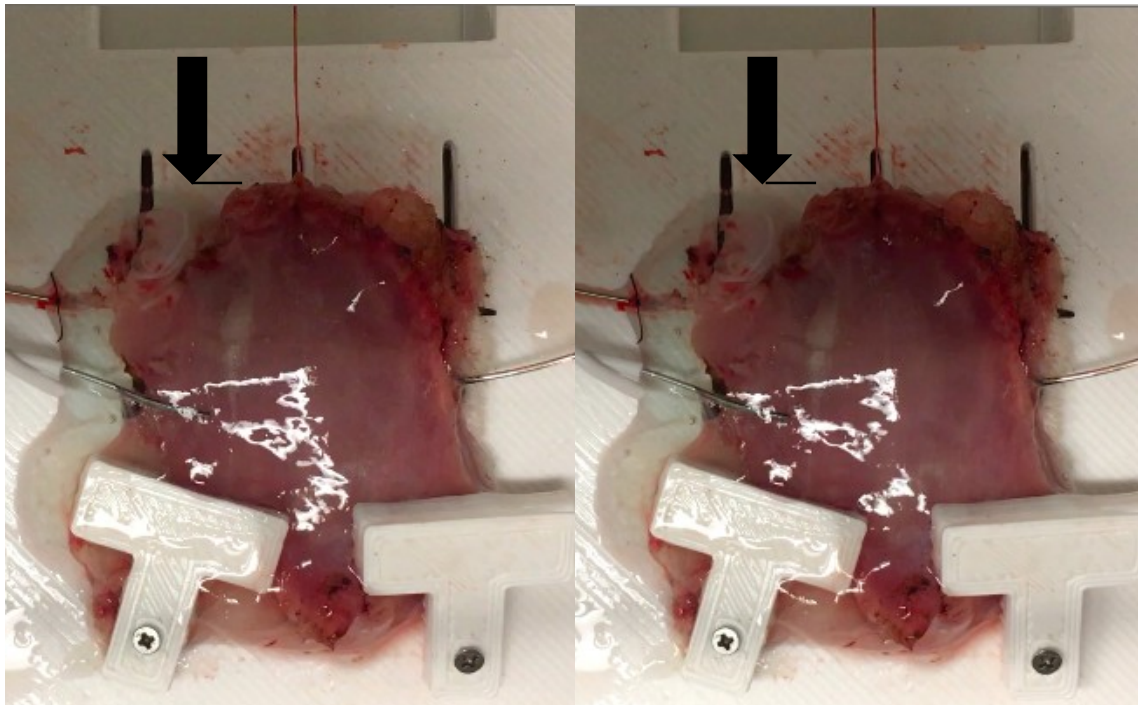


Figure 5.8 Experiment 2: Frames of the Tissue when Unstimulated (Left) and Stimulated (Right)

Figure 5.9 shows the measurements taken by the force sensor. Unfortunately, since the contraction was very small and limited to the top left corner, the force sensor was unable to read any force changes due to its site of attachment to the tissue.

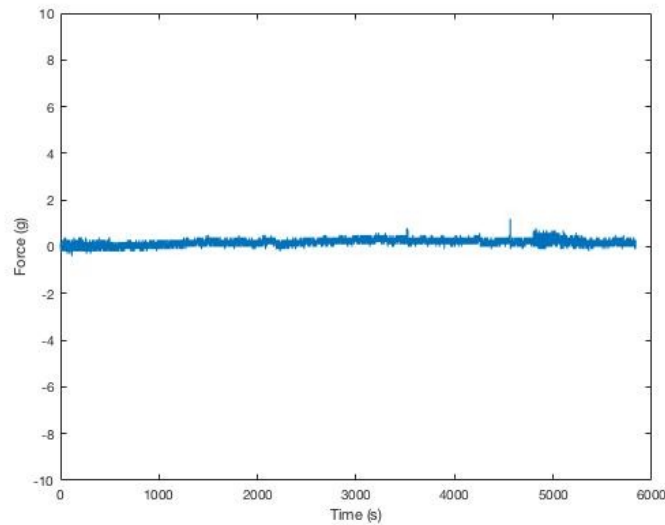


Figure 5.9 Experiment 2: Force Measurement Readings

5.5 Discussion

The goal of this section was to develop a system that is capable of stimulating the rat abdominal walls to contract. At first, the H-Bridge circuit was designed and implemented in order to be able to convert a direct current into alternating current of any specific frequency. That alternating current is then used to provide biphasic electrical stimulation to the rat abdominal wall. As mentioned before, biphasic stimulation is preferred over monophasic stimulation due to biphasic stimulation being able to maintain the ion concentration in the tissue thus avoiding tissue damage.

Experiment 1 served as a proof of concept that the electrical stimulation system could be used to stimulate the rat abdominal wall and elicit a contraction from it. Since the force sensor was not available to use for this, a video was used to record the stimulation and a MATLAB script was used analyze the video frames. It showed that the electrical stimulation system was able to stimulate the rat abdominal wall and cause a contraction.

Experiment 2 served as a test to determine whether or not the electrical stimulation system could be incorporated into the bioreactor prototype. Even though the force sensors were

unable to sense any forces caused by the tissue's contractions, this experiment should still be considered a success because as seen in **Figure 5.8**, the tissue is still able to contract, even though it is a very small amount. This is probably due to the fact that the tissue was not perfused and stimulated immediately after the harvest surgery until about two hours later. If the bioreactor was set up properly and the tissue was stimulated almost immediately after harvesting, as seen in Experiment 1, the tissue would have contracted enough for the force sensor to read it.

Overall, these two experiments are useful because it shows they help define a time limit on how long the abdominal wall is able to sit after its edges are cauterized even if the vessels are connected as well as give information to design a better connector between the abdominal wall and force sensor. Instead of anchoring the force sensor to the tissue with a thread at a single point, a scaffold can be designed to attach to the tissue at multiple points with sutures. Afterwards, that scaffold can be attached to the force sensor to allow it to sense any force changes regardless of its position.

CHAPTER 6: CONCLUSIONS

This project focused on developing a bioreactor for normothermic perfusion of rat abdominal wall VCA. The rat abdominal wall was used as the VCA model for this project because abdominal wall transplants are the second most common type of VCA. Even though there are commercialized perfusion systems for organ preservation, there are no specific systems for VCA.

By combining normothermic perfusion and electrical stimulation, the preservation times of VCA can hopefully be extended from the current gold standards of 4-6 hours up to 12 hours and eventually 72 hours. In addition, various inline sensors are incorporated to help monitor the health and status of the graft. Once the nitric oxide, reactive oxygen species, glucose, and lactate inline sensors have been developed by our collaborators, they can be easily incorporated into the bioreactor system.

The bioreactor was designed to accommodate the abdominal wall VCA, the perfusion system, and the electrical stimulation system. A prototype was 3D printed with ABS plastic and used for testing. The prototype was able to store the abdominal wall and simultaneously allows for both perfusion and electrical stimulation of the abdominal wall.

Throughout the tests, valuable data and insight was obtained in order to better inform the design for the next iteration of the bioreactor. For example, a different method of clamping the abdominal wall to the bioreactor and force sensor should be designed since the current method only anchors the force sensor to a single point on the tissue and is unreliable. In addition, future testing and calibration should be done with the sensor to increase their reliability.

But overall, this bioreactor was able to both perfuse and electrically stimulate the rat abdominal wall. This allows for the study of different methods to extend the preservation time of

this VCA model, such as changing the electrical stimulation regime or adding different components to the perfusate. Eventually, once the abdominal wall VCA's preservation times have been extended to a satisfactory time, this bioreactor can be easily modified to accommodate the next model for the project: rat forelimb VCA.

REFERENCES

- [1] T. Schlich, “The origins of organ transplantation,” *Lancet (London, England)*, vol. 378, no. 9800, pp. 1372–3, Oct. 2011.
- [2] P. K. Linden, “History of Solid Organ Transplantation and Organ Donation,” *Crit. Care Clin.*, vol. 25, no. 1, pp. 165–184, Jan. 2009.
- [3] C. N. Barnard, “The operation: a human cardiac transplant: an interim report of a successful operation performed at Groote Schuur Hospital,” *SAMJ South African Med. J.*, vol. 107, no. 12, pp. 1271–1274, 2017.
- [4] R. Girlanda, “Deceased organ donation for transplantation: Challenges and opportunities,” *World J. Transplant.*, vol. 6, no. 3, pp. 451–9, Sep. 2016.
- [5] D. E. Stewart, V. C. Garcia, J. D. Rosendale, D. K. Klassen, and B. J. Carrico, “Diagnosing the Decades-Long Rise in the Deceased Donor Kidney Discard Rate in the United States,” *Transplantation*, vol. 101, no. 3, pp. 575–587, Mar. 2017.
- [6] “Matching Donors & Recipients: The Organ Matching Process | organdonor.gov.” [Online]. Available: <https://organdonor.gov/about/process/matching.html>. [Accessed: 30-Mar-2018].
- [7] L. C. Cendales, J. Kanitakis, and C. Burns, “Vascularized Composite Allotransplantation,” in *Pathology of Solid Organ Transplantation*, Berlin, Heidelberg: Springer Berlin Heidelberg, 2009, pp. 393–399.
- [8] E. J. Caterson, J. Lopez, M. Medina, B. Pomahac, and S. G. Tullius, “Ischemia-Reperfusion Injury in Vascularized Composite Allotransplantation,” *J. Craniofac. Surg.*, vol. 24, no. 1, pp. 51–56, Jan. 2013.
- [9] M. Kueckelhaus *et al.*, “A mobile extracorporeal extremity salvage system for replantation and transplantation,” *Ann. Plast. Surg.*, vol. 76, no. 3, pp. 355–360, 2016.
- [10] K. Azari and G. Brandacher, “Vascularized composite allotransplantation,” *Curr. Opin. Organ Transplant.*, p. 1, Nov. 2013.
- [11] N. Krezdorn *et al.*, “Tissue conservation for transplantation,” *Innov Surg Sci*, vol. 2, no. 4, pp. 171–187, 2017.
- [12] H. K. Eltzschig and T. Eckle, “Ischemia and reperfusion—from mechanism to translation,” *Nat. Med.*, vol. 17, no. 11, pp. 1391–1401, Nov. 2011.
- [13] F. Shimizu, O. Okamoto, K. Katagiri, S. Fujiwara, and F.-C. Wei, “Prolonged ischemia increases severity of rejection in skin flap allotransplantation in rats,” *Microsurgery*, vol. 30, no. 2, p. NA-NA, 2010.

- [14] P. a Clavien, P. R. Harvey, and S. M. Strasberg, "Preservation and reperfusion injuries in liver allografts. An overview and synthesis of current studies.," *Transplantation*, vol. 53, no. 5. pp. 957–78, 1992.
- [15] E. E. Guibert, A. Y. Petrenko, C. L. Balaban, A. Y. Somov, J. V Rodriguez, and B. J. Fuller, "Organ Preservation: Current Concepts and New Strategies for the Next Decade.," *Transfus. Med. Hemother.*, vol. 38, no. 2, pp. 125–142, 2011.
- [16] J. Erhard *et al.*, "Comparison of histidine-tryptophan-ketoglutarate (HTK) solution versus University of Wisconsin (UW) solution for organ preservation in human liver transplantation," *Transpl Int*, vol. 7, pp. 177–181, 1994.
- [17] X. Yuan *et al.*, "Machine perfusion or cold storage in organ transplantation: indication, mechanisms, and future perspectives," *Transpl. Int.*, vol. 23, no. 6, pp. 561–570, Jan. 2010.
- [18] A. Carrel and C. A. Lindbergh, "The Culture of Whole Organs," *Source Sci. New Ser.*, vol. 81, no. 21, pp. 621–623, 1935.
- [19] J. Brockmann *et al.*, "Normothermic perfusion: A new paradigm for organ preservation," *Ann. Surg.*, vol. 250, no. 1, pp. 1–6, 2009.
- [20] "Understanding Blood Pressure Readings." [Online]. Available: http://www.heart.org/HEARTORG/Conditions/HighBloodPressure/KnowYourNumbers/Understanding-Blood-Pressure-Readings_UCM_301764_Article.jsp. [Accessed: 29-Mar-2018].
- [21] R. Ravikumar *et al.*, "Liver Transplantation After Ex Vivo Normothermic Machine Preservation: A Phase 1 (First-in-Man) Clinical Trial."
- [22] W. Hassanein, "Systems and methods for ex-vivo organ care," 07-Oct-2005.
- [23] "Organ Transport Systems | Our Technology." [Online]. Available: <http://www.organtransportsystems.com/OurTechnology.html>. [Accessed: 29-Mar-2018].
- [24] M. Cobert, M. Peltz, L. West, and M. E. Jessen, "174: Maintenance of Human Heart Oxidative Metabolism after 12 Hour Perfusion Preservation," *J. Hear. Lung Transplant.*, vol. 28, no. 2, pp. S126–S127, Feb. 2009.
- [25] "Paragonix Sherpa™ Organ Transport Systems." [Online]. Available: <http://paragonixtechnologies.com/>. [Accessed: 29-Mar-2018].
- [26] "OCS Heart system for heart transplant | Guidance and guidelines | NICE." [Online]. Available: <https://www.nice.org.uk/advice/mib86/chapter/the-technology>. [Accessed: 29-Mar-2018].
- [27] "Organ Assist - Organ Perfusion Systems - Lung Assist." [Online]. Available: <https://www.organ-assist.nl/products/lung-assist>. [Accessed: 29-Mar-2018].

- [28] R. Fishman, “Systems and methods for ex vivo lung care,” 08-Apr-2008.
- [29] “XVIVO Perfusion | XPS™ - XVIVO Perfusion.” [Online]. Available: <http://www.xvivoperfusion.com/products/xps/>. [Accessed: 29-Mar-2018].
- [30] “LifePort® Kidney Transporter 1.0 | Organ Recovery Systems.” [Online]. Available: <https://www.organ-recovery.com/lifeport-kidney-transporter/lifeport-kidney-transporter-1.0>. [Accessed: 29-Mar-2018].
- [31] “Organ Assist - Organ Perfusion Systems - Kidney Assist-transport.” [Online]. Available: https://www.organ-assist.nl/products/kidney-assist__transport#producten. [Accessed: 29-Mar-2018].
- [32] “Waves – WTRS.” [Online]. Available: <http://wtrs.com/portfolio/waves/>. [Accessed: 29-Mar-2018].
- [33] “RM3 – WTRS.” [Online]. Available: <http://wtrs.com/portfolio/rm3/>. [Accessed: 29-Mar-2018].
- [34] “LifePort Liver Transporter | Organ Recovery Systems.” [Online]. Available: <https://www.organ-recovery.com/lifeport-liver-transporter>. [Accessed: 29-Mar-2018].
- [35] “Organ Assist - Organ Perfusion Systems - Liver Assist.” [Online]. Available: <https://www.organ-assist.nl/products/liver-assist>. [Accessed: 29-Mar-2018].
- [36] “OrganOx Metra.” [Online]. Available: <http://www.organox.com/metra>. [Accessed: 29-Mar-2018].
- [37] “TransMedics Announces The World’s First Human Liver Transplantation Using The Organ Care System (OCS™) Liver Technology & The Initiation of The OCS™ Liver PROTECT U.S. Pivotal Trial: TransMedics, Inc.” [Online]. Available: http://www.transmedics.com/wt/page/pr_1456236855.html. [Accessed: 29-Mar-2018].
- [38] W. Hassanein, “Ex vivo organ care system,” 02-Jun-2015.
- [39] M. Kueckelhaus *et al.*, “Acellular Hypothermic Extracorporeal Perfusion Extends Allowable Ischemia Time in a Porcine Whole Limb Replantation Model,” *Plast. Reconstr. Surg.*, vol. 139, no. 4, p. 922e–932e, 2017.
- [40] K. Ozer, A. Rojas-Pena, C. L. Mendias, B. Bryner, C. Toomasian, and R. H. Bartlett, “Ex situ limb perfusion system to extend vascularized composite tissue allograft survival in Swine,” *Transplantation*, vol. 99, no. 10, pp. 2095–2101, 2015.
- [41] K. Ozer, A. Rojas-Pena, C. L. Mendias, B. S. Bryner, C. Toomasian, and R. H. Bartlett, “The effect of ex situ perfusion in a swine limb vascularized composite tissue allograft on survival up to 24 hours,” *J. Hand Surg. Am.*, vol. 41, no. 1, pp. 3–12, 2016.
- [42] N. L. Werner *et al.*, “Ex situ perfusion of human limb allografts for 24 hours,”

Transplantation, vol. 101, no. 3, pp. e68–e74, 2017.

- [43] J. M. Broyles *et al.*, “Reconstruction of Large Abdominal Wall Defects Using Neurotized Vascular Composite Allografts,” *Plast. Reconstr. Surg.*, vol. 136, no. 4, pp. 728–737, Oct. 2015.
- [44] S. H. M. Brown and S. M. McGill, “Transmission of muscularly generated force and stiffness between layers of the rat abdominal wall,” *Spine (Phila. Pa. 1976)*, vol. 34, no. 2, pp. 70–75, 2009.
- [45] F. Kolář and L. Janský, “Oxygen consumption in rat skeletal muscle at various rates of oxygen delivery,” *Experientia*, vol. 40, no. 4, pp. 353–354, Apr. 1984.
- [46] J. Son, D. Lee, and Y. Kim, “Effects of involuntary eccentric contraction training by neuromuscular electrical stimulation on the enhancement of muscle strength,” *Clin. Biomech.*, vol. 29, no. 7, pp. 767–772, Aug. 2014.
- [47] M. P. Willand, M. Holmes, J. R. Bain, M. Fahnestock, and H. De Bruin, “Electrical muscle stimulation after immediate nerve repair reduces muscle atrophy without affecting reinnervation,” *Muscle Nerve*, vol. 48, no. 2, pp. 219–225, Aug. 2013.
- [48] R. Jung, K. Ichihara, G. Venkatasubramanian, and J. J. Abbas, “Chronic neuromuscular electrical stimulation of paralyzed hindlimbs in a rodent model,” *J. Neurosci. Methods*, vol. 183, no. 2, pp. 241–254, Oct. 2009.
- [49] J. A. Balogun, O. O. Onilari, O. A. Akeju, and D. K. Marzouk, “High Voltage Electrical Stimulation in the Augmentation Muscle Strength: Effects of Pulse Frequency.”
- [50] M. P. Willand, J. P. Lopez, H. de Bruin, M. Fahnestock, M. Holmes, and J. R. Bain, “A new system and paradigm for chronic stimulation of denervated rat muscle,” *J. Med. Biol. Eng.*, vol. 31, no. 2, pp. 87–92, 2011.

APPENDICES

List of Materials for Bioreactor

- 1x Base
- 1x Left Wall
- 1x Right Wall
- 1x Back Wall
- 1x Top Cover
- 1x Perfusate Drainage Reservoir
- 1x Tissue Clamp Platform
- 2x Back Panels
- 1x Front Panel
- 1x Top Panel
- 2x Clamps
- 1x Ismatec IP8 8 Channel Peristaltic Pump
- 1x 16/35 PowerLab
- 2x FE221 Bridge Amplifier
- 1x MLT1030/D Force Transducer
- 1x MLT1199 Pressure Transducer
- 2x 8-730 Flow-Through Oxygen Probes
- 2x O2-ADPT100-BNC O2 Adaptor
- 2x MLT1402 T-Type Thermocouples
- 2x T-Type Pods
- 2x 8-705 Flow-Through pH Probes
- 2x 8-702 Flow-Through pH Reference Electrodes
- 2x MV-ADPT-BNC Millivolt Adaptors
- 2x Electrode Tab
- 2x Electrode Screw
- 26x 0/80 x 3/8 Phillips Flat Machine Screws
- 10x Female Luer Locks
- 10x Male Luer Locks
- 1x Glass Media Bottle
- 1x TP3005T Power Supply
- 1x Arduino Uno Microcontroller
- 1x Circuit Prototyping Board
- 2x FQP27P06 P-Channel MOSFETs
- 2x FQP30N06L N-Channel MOSFETs
- 2x BC33716BU NPN Transistors
- 4x 20k Ω Resistors
- 4x 1.5k Ω Resistors
- 1x Electronix Express Solid Wire Kit

Arduino Code: Electrical Stimulation

```
long double frequency = 70.0; //Hz
long double x = 1000.0 / (frequency * 2.0);
//x = half period in ms
long double period = x * 2.0;

long double num_runs = 300.0 / period; //300 for 300ms
void setup()
{
  pinMode(13, OUTPUT);
  pinMode(11, OUTPUT);
  digitalWrite(11, LOW);
  digitalWrite(13, LOW);
}

void loop()
{
  delay(4.7*1000);
  //300ms Pulse of x frequency
  for(int i = 1; i <= num_runs; i = i + 1 )
  {
    digitalWrite(11, LOW);
    digitalWrite(13, HIGH);
    delayMicroseconds(x*1000);
    digitalWrite(13, LOW);
    digitalWrite(11, HIGH);
    delayMicroseconds(x*1000);
  }
  digitalWrite(13, LOW); //Setting everything low again
  digitalWrite(11, LOW);
```

MATLAB Code: Measuring the Percent Area of Contraction Upon Stimulation

```
clc
clear

str1 = 'IMG_74';
str3 = '.m4v';

video = 1;

for i = [23:25]
  str2 = int2str(i);
  string = strcat(str1, str2, str3);
  x = VideoReader(string);
```

```

    frame = 1;
while hasFrame(x)
    I1 = readFrame(x); %Get the frame from the video
    I2 = imcrop(I1,[130 400 750 850]); % xstart ystart xsteps ysteps
    I3 = rgb2gray(I2);
    %I4 = imbinarize(I3);

    I4 = I3;
    for r = 1:851
        for c = 1:751
            if I4(r,c) >= 120
                I4(r,c) = 255;
            else
                I4(r,c) = 0;
            end
        end
    end
end

total(frame, video) = bwarea(I4); %measures white area
subplot(1,4,1);
imshow(I1);
subplot(1,4,2);
imshow(I2);
subplot(1,4,3);
imshow(I3);
subplot(1,4,4);
imshow(I4);

    frame = frame+1
end

video = video + 1
end

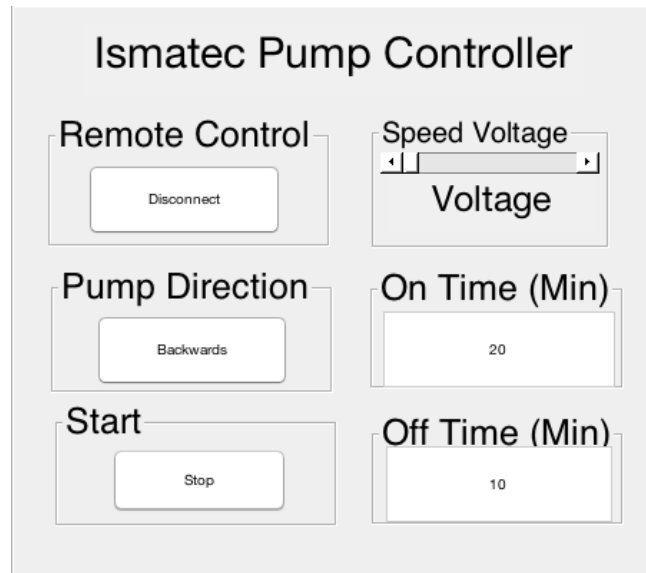
num = 1;
for i = 1:3
    stuff(i, 1) = max(total(:,i));
    temp = total(:,i);
    stuff(i, 2) = min(temp(temp>0));

    stuff(i, 3) = (stuff(i,1)-stuff(i,2)) / stuff(i,i) * 100;
end

save('data.txt','total','-ascii')
save('stuff.txt','stuff','-ascii')

```


MATLAB Code & GUI: Automation of the Pump



```
function varargout = Pump_GUI(varargin)
% PUMP_GUI MATLAB code for Pump_GUI.fig
%   PUMP_GUI, by itself, creates a new PUMP_GUI or raises the existing
%   singleton*.
%
%   H = PUMP_GUI returns the handle to a new PUMP_GUI or the handle to
%   the existing singleton*.
%
%   PUMP_GUI('CALLBACK',hObject,eventData,handles,...) calls the local
%   function named CALLBACK in PUMP_GUI.M with the given input arguments.
%
%   PUMP_GUI('Property','Value',...) creates a new PUMP_GUI or raises the
%   existing singleton*. Starting from the left, property value pairs are
%   applied to the GUI before Pump_GUI_OpeningFcn gets called. An
%   unrecognized property name or invalid value makes property application
%   stop. All inputs are passed to Pump_GUI_OpeningFcn via varargin.
%
%   *See GUI Options on GUIDE's Tools menu. Choose "GUI allows only one
%   instance to run (singleton)".
%
% See also: GUIDE, GUIDATA, GUIHANDLES

% Edit the above text to modify the response to help Pump_GUI

% Last Modified by GUIDE v2.5 29-Nov-2017 15:23:21

% Begin initialization code - DO NOT EDIT
gui_Singleton = 1;
gui_State = struct('gui_Name',       mfilename, ...
                  'gui_Singleton',   gui_Singleton, ...
                  'gui_OpeningFcn', @Pump_GUI_OpeningFcn, ...
                  'gui_OutputFcn',  @Pump_GUI_OutputFcn, ...
                  'gui_LayoutFcn',  [], ...
                  'gui_Callback',    []);
if nargin && ischar(varargin{1})
```

```

    gui_State.gui_Callback = str2func(varargin{1});
end

if nargin
    [varargout{1:nargout}] = gui_mainfcn(gui_State, varargin{:});
else
    gui_mainfcn(gui_State, varargin{:});
end
% End initialization code - DO NOT EDIT

% --- Executes just before Pump_GUI is made visible.
function Pump_GUI_OpeningFcn(hObject, eventdata, handles, varargin)
% This function has no output args, see OutputFcn.
% hObject    handle to figure
% eventdata  reserved - to be defined in a future version of MATLAB
% handles     structure with handles and user data (see GUIDATA)
% varargin    command line arguments to Pump_GUI (see VARARGIN)

% Choose default command line output for Pump_GUI
handles.output = hObject;

% Update handles structure
guidata(hObject, handles);

% UIWAIT makes Pump_GUI wait for user response (see UIRESUME)
% uiwait(handles.figure1);

%Connecting Matlab to Arduino
disp('Setting up Arduino Settings... Please wait...');
%handles.text_status.String = ['Setting up Arduino Settings... Please
wait...'];
delete(instrfind({'Port'}, {'/dev/cu.usbmodem1421'}))
clear a;
global a
a = arduino('/dev/cu.usbmodem1421', 'Uno')
disp('The Arduino is now ready.');
```

```

voltage = get(handles.slider_voltage, 'Value');
handles.text_voltage.String = [num2str(voltage)];

handles.push_connect.Visible = 'on';
handles.push_forward.Visible = 'off';
handles.push_stop.Visible = 'off';

handles.push_disconnect.Visible = 'off';
handles.push_backwards.Visible = 'on';
handles.push_run.Visible = 'on';

global runFlag %0 means pump is stopped
runFlag = 0;
%Default Values
writeDigitalPin(a, 'D2', 1); %Pin2: 1 = Pump, 0 = Remote
writeDigitalPin(a, 'D4', 1); %Pin4: 1 = Clockwise, 0 = Counterclockwise
writeDigitalPin(a, 'D3', 1); %Pin3: 1 = Stop, 0 = Run
writeDigitalPin(a, 'D5', 0);

```

```

writeDigitalPin(a, 'D13', 0); %Pin 13: 0 = Control speed via panel
%writePWMPVltage(a, 'D5', 0);

% --- Outputs from this function are returned to the command line.
function varargout = Pump_GUI_OutputFcn(hObject, eventdata, handles)
% varargout cell array for returning output args (see VARARGOUT);
% hObject handle to figure
% eventdata reserved - to be defined in a future version of MATLAB
% handles structure with handles and user data (see GUIDATA)

% Get default command line output from handles structure
varargout{1} = handles.output;

% --- Executes on button press in push_run.
function push_run_Callback(hObject, eventdata, handles)
% hObject handle to push_run (see GCBO)
% eventdata reserved - to be defined in a future version of MATLAB
% handles structure with handles and user data (see GUIDATA)

global a;
global runFlag;

handles.push_run.Visible = 'off';
handles.push_stop.Visible = 'on';
onTime = str2num(get(handles.edit_on, 'String'))
offTime = str2num(get(handles.edit_off, 'String'))

runFlag = 1;
disp('Pump started');

while (runFlag == 1)
    writeDigitalPin(a, 'D3', 0);
    pause(onTime*60);

    if offTime ~= 0
        writeDigitalPin(a, 'D3', 1);
        pause(offTime*60);
    end
end

% --- Executes on button press in push_stop.
function push_stop_Callback(hObject, eventdata, handles)
% hObject handle to push_stop (see GCBO)
% eventdata reserved - to be defined in a future version of MATLAB
% handles structure with handles and user data (see GUIDATA)
global a
global runFlag
handles.push_run.Visible = 'on';
handles.push_stop.Visible = 'off';
writeDigitalPin(a, 'D3', 1);
runFlag = 0;
disp('Pump stopped');

```

```

% --- Executes on button press in push_forward.
function push_forward_Callback(hObject, eventdata, handles)
% hObject      handle to push_forward (see GCBO)
% eventdata    reserved - to be defined in a future version of MATLAB
% handles      structure with handles and user data (see GUIDATA)
global a
handles.push_forward.Visible = 'off';
handles.push_backwards.Visible = 'on';
writeDigitalPin(a, 'D4', 1);
disp('Pump set to Forward');

% --- Executes on button press in push_backwards.
function push_backwards_Callback(hObject, eventdata, handles)
% hObject      handle to push_backwards (see GCBO)
% eventdata    reserved - to be defined in a future version of MATLAB
% handles      structure with handles and user data (see GUIDATA)
global a
handles.push_forward.Visible = 'on';
handles.push_backwards.Visible = 'off';
writeDigitalPin(a, 'D4', 0);
disp('Pump set to Backwards');

% --- Executes on button press in push_connect.
function push_connect_Callback(hObject, eventdata, handles)
% hObject      handle to push_connect (see GCBO)
% eventdata    reserved - to be defined in a future version of MATLAB
% handles      structure with handles and user data (see GUIDATA)
global a
handles.push_disconnect.Visible = 'on';
handles.push_connect.Visible = 'off';
writeDigitalPin(a, 'D2', 0);
disp('Remote control is on');

% --- Executes on button press in push_disconnect.
function push_disconnect_Callback(hObject, eventdata, handles)
% hObject      handle to push_disconnect (see GCBO)
% eventdata    reserved - to be defined in a future version of MATLAB
% handles      structure with handles and user data (see GUIDATA)
global a
handles.push_disconnect.Visible = 'off';
handles.push_connect.Visible = 'on';
writeDigitalPin(a, 'D2', 1);
disp('Remote control is off');

% --- Executes on slider movement.
function slider_voltage_Callback(hObject, eventdata, handles)
% hObject      handle to slider_voltage (see GCBO)
% eventdata    reserved - to be defined in a future version of MATLAB
% handles      structure with handles and user data (see GUIDATA)

% Hints: get(hObject,'Value') returns position of slider
%        get(hObject,'Min') and get(hObject,'Max') to determine range of

```

```

slider
voltage = get(handles.slider_voltage, 'Value')
handles.text_voltage.String = [num2str(voltage)];

global a;
%a.analogWrite(5,voltage);
writePWMPWMVoltage(a, 'D5', voltage);

% --- Executes during object creation, after setting all properties.
function slider_voltage_CreateFcn(hObject, eventdata, handles)
% hObject    handle to slider_voltage (see GCBO)
% eventdata  reserved - to be defined in a future version of MATLAB
% handles    empty - handles not created until after all CreateFcns called

% Hint: slider controls usually have a light gray background.
if isequal(get(hObject, 'BackgroundColor'),
get(0, 'defaultUiControlBackgroundColor'))
    set(hObject, 'BackgroundColor', [.9 .9 .9]);
end

function edit_off_Callback(hObject, eventdata, handles)
% hObject    handle to edit_off (see GCBO)
% eventdata  reserved - to be defined in a future version of MATLAB
% handles    structure with handles and user data (see GUIDATA)

% Hints: get(hObject, 'String') returns contents of edit_off as text
%        str2double(get(hObject, 'String')) returns contents of edit_off as a
double

% --- Executes during object creation, after setting all properties.
function edit_off_CreateFcn(hObject, eventdata, handles)
% hObject    handle to edit_off (see GCBO)
% eventdata  reserved - to be defined in a future version of MATLAB
% handles    empty - handles not created until after all CreateFcns called

% Hint: edit controls usually have a white background on Windows.
%        See ISPC and COMPUTER.
if ispc && isequal(get(hObject, 'BackgroundColor'),
get(0, 'defaultUiControlBackgroundColor'))
    set(hObject, 'BackgroundColor', 'white');
end

function edit_on_Callback(hObject, eventdata, handles)
% hObject    handle to edit_on (see GCBO)
% eventdata  reserved - to be defined in a future version of MATLAB
% handles    structure with handles and user data (see GUIDATA)

% Hints: get(hObject, 'String') returns contents of edit_on as text
%        str2double(get(hObject, 'String')) returns contents of edit_on as a

```

```
double
```

```
% --- Executes during object creation, after setting all properties.
function edit_on_CreateFcn(hObject, eventdata, handles)
% hObject    handle to edit_on (see GCBO)
% eventdata  reserved - to be defined in a future version of MATLAB
% handles    empty - handles not created until after all CreateFcns called

% Hint: edit controls usually have a white background on Windows.
%       See ISPC and COMPUTER.
if ispc && isequal(get(hObject,'BackgroundColor'),
get(0,'defaultUicontrolBackgroundColor'))
    set(hObject,'BackgroundColor','white');
end
```

CURRICULUM VITAE

Kenny Tran

9714 Peach Tree Ln. Rowlett, TX 75089
214-218-5711 | Kenny.tran81794@gmail.com

EDUCATION

2016-2018

Master of Science and Engineering in Biomedical Engineering (MSE)

Johns Hopkins University, Baltimore MD

GPA: 3.4

Relevant Coursework: Cellular Engineering, Tissue Engineering, Cell and Tissue Engineering Lab, Microfabrication Lab, Principles of the Design of Biomedical Instrumentation, Systems Bioengineering I & II

2012-2016

Bachelor of Science in Biomedical Engineering (BS)

University of Texas at Dallas, Richardson TX

GPA: 3.938

Honors: Magna Cum Laude, Deans List 2013-2015, Tau Beta Xi Member

Relevant Coursework: Intro to Modern Biology, Biology Lab, Engineering Physiology of the Human Body + Lab, Advanced Engineering Physiology, Quantitative Cell Biology, Electrical/Electronic Circuits, Biomedical Circuits/Instrumentation Lab, Signals and Systems + Lab, Digital Circuits, Advanced MATLAB Programming, Feedback Systems + Lab, Thermodynamics, Biomaterials & Medical Devices, Bioelectric Systems, Statics and Dynamics, Differential Equations, Linear Algebra, Advanced Engineering Math, Probability and Statistics

RESEARCH EXPERIENCE

Masters/Graduate Researcher

January 2017 – June 2018

Grayson Lab for Craniofacial and Orthopaedic Tissue Engineering

Johns Hopkins University, Baltimore MD

Dr. Warren L. Grayson, Ph.D., Professor of Biomedical Engineering